Koglin, N., Zeh, A., Franz, G., Schüssler, U., Glodny, J., Gerdes, A., Brätz, H. (2018): From Cadomian magmatic arc to Rheic ocean closure: The geochronological-geochemical record of nappe protoliths of the Münchberg Massif, NE Bavaria (Germany). - *Gondwana Research*, *55*, pp. 135—152.

DOI: http://doi.org/10.1016/j.gr.2017.11.001

From Cadomian magmatic arc to Rheic ocean closure: The geochronological-geochemical record of nappe protoliths of the Münchberg Massif, NE Bavaria (Germany)

Nikola Koglin[a], Armin Zeh[b], Gerhard Franz[c], Ulrich Schüssler[a], Johannes Glodny[d], Axel Gerdes[e], Helene Brätz[f]

[a] Geodynamics and Geomaterials Research Division, Institute of Geography and Geology, University of Würzburg, Am Hubland, 97074 Würzburg, Germany

nikola.koglin@uni-wuerzburg.de, uli.schuessler@uni-wuerzburg.de

[b] KIT Karlsruher Institut für Technologie, Angewandte Geowissenschaften - Mineralogie und Petrologie, Adenauerring 20b, Geb. 50.40, 76131 Karlsruhe, Germany

armin.zeh@kit.edu

[c] Institute for Applied Geosciences, Ackerstrasse 76, 13355 Berlin, Germany

gerhard.franz@tu-berlin.de

[d] GFZ German Research Centre for Geosciences, Telegrafenberg, 14473 Potsdam, Germany

johannes.glodny@gfz-potsdam.de

[e] Institute for Geosciences, University of Frankfurt, Altenhöferallee 1, 60438 Frankfurt/Main, Germany

gerdes@em.uni-frankfurt.de

[f] Geo-Center of Northern Bavaria, University of Erlangen, Schlossgarten 5, 91054 Erlangen, Germany

helene.braetz@fau.de

Corresponding author E-mail: nikola.koglin@uni-wuerzburg.de

Abstract

The Münchberg Massif in northeastern Bavaria, Germany is an allochthonous metamorphic nappe complex within the Saxothuringian Zone of the Variscan orogen. From top to bottom it consists of four major units: Hangend-Serie, Liegend-Serie, Randamphibolit-Serie and Prasinit-Phyllit-Serie, which show an inverted metamorphic gradient of eclogite- to amphibolite-facies (top) to greenschist-facies (bottom) and are separated from each other by thrust faults. New geochemical and U-Pb zircon data indicate that the four units host metasedimentary and meta-igneous rocks which were formed at different time and in distinct geotectonic settings during the evolution of the Saxothuringian terrane between 550 and 370 Ma. Mafic and felsic protoliths of the **Hangend-Serie** result from a bimodal magmatism in an evolved oceanic to continental magmatic arc setting at about 550 Ma. These rocks represent relics of the Cadomian magmatic arc, which formed a cordillera at the northern margin of Gondwana during the Neoproterozoic. The **Liegend-Serie** hosts slivers of granitic orthogneisses, emplaced during magmatic events at c. 505 and 480 Ma, and Early Palaeozoic paragneisses, with our samples deposited at ≤ 483 Ma. Ortho- and paragneisses were affected by an amphibolite-facies metamorphic overprint at c. 380 Ma. Granite emplacement and sediment deposition can be related to the separation of the Avalonia microterrane from the northern Gondwana margin. Amphibolite protoliths of the **Randamphibolit-Serie** emplaced at c. 400 Ma. They show MORB to E-MORB signatures, pointing to their formation along an oceanic spreading centre within the Rheic ocean. Mafic igneous rocks in the **Prasinit-Phyllit-Serie** emplaced at nearly the same time (407-401 Ma), but their calc-alkaline to tholeiitic character rather suggests formation in an intra-oceanic island arc / back arc system. This convergent margin lasted for about 30 Ma until the Late Devonian, as is suggested by a maximum deposition age of 371 Ma of associated phyllites, and by metamorphic Ar-Ar ages of 374-368 Ma. The timing of the different magmatic and sedimentary events in the Münchberg Massif and their plate tectonic settings are similar to those estimated for other Variscan nappe complexes throughout Europe, comprising the French Massif Central and NW Spain. This similarity indicates that the Münchberg Massif forms part of a European-wide suture zone, along which rock units of different origin were assembled in a complex way during the Variscan Orogeny.

Keywords

Münchberg Massif; Saxothuringian Zone; Cadomian-Variscan evolution; geochemistry; zircon ages

1 Introduction

The Saxothuringian Zone in Germany forms part of the Variscan orogenic belt, extending from Spain in the west to Poland to the east (Fig. 1), and is made up by a remarkable variety of lithological and geotectonic units, ranging in age from Late Proterozoic to Early Carboniferous. For reconstruction of the evolution of the Saxothuringian Zone and its wider role within the European Variscan belt, detailed knowledge about the timing of geological processes, and the original positions and geotectonic settings of all units involved is essential. One important unit within the Saxothuringian is the Münchberg Massif in northeastern Bavaria. This massif hosts a pile of four nappe units characterised by different metamorphic grades, from amphibolite-facies and, in part, eclogite-facies on top to low-grade metamorphic conditions at the base. Previous studies about the Münchberg Massif focused mainly on the timing of the metamorphic overprint (e.g. Stosch and Lugmair 1990; Kreuzer et al. 1989; Scherer et al. 2002), on preliminary geochemical classification of mainly metabasitic rocks (e.g. Okrusch et al. 1989), and on *P*-*T* path reconstructions of the eclogites (e.g. Franz et al. 1986; Klemd 1989), whereas information about the timing of sediment deposition and magma intrusions, as well as about geotectonic settings and sediment provenances are very scarce. Presently, there is only one Rb-Sr whole rock isochrone age of 482 ± 20 Ma of an augengneiss from the Liegend-Serie (Söllner et al. 1981), whereas the nature and age of most ortho- and paragneisses of the Münchberg Massif are completely unknown.

In order to fill this gap of knowledge, new whole rock geochemical analyses and U-Pb zircon ages, representative for each of the four metamorphic nappes, are presented. These data provide new information about magmatic protolith ages, maximum deposition ages, geotectonic settings, and the provenances of the (meta)sedimentary rocks. In combination they will also place new constraints on the evolution of the Saxothuringian Zone, and allow detailed comparisons with other basement units throughout Europe formed between the Neoproterozoic to Late Devonian.

2 Geological setting, sampling and petrography

The Münchberg Massif forms part of the Saxothuringian Zone in Germany (Fig. 1). It consists of four major units, which are designated (from top to bottom): the Hangend-Serie (“hanging-wall series”), the Liegend-Serie (“footwall series”), the Randamphibolit-Serie (“marginal-amphibolite series”) and the Prasinit-Phyllit-Serie (“greenschist-phyllite series”) (Stettner 1960a). After decades of controversial discussion, there is now general consensus that these four units represent remnants of a previously much larger nappe complex, comprising the Münchberg Massif, the Frankenberg and Wildenfels klippen complexes, and at least parts of the Teplá-Barrandian block (e.g. Franke et al. 2017). The Münchberg Massif superposes very low-grade Palaeozoic metasedimentary sequences of the Frankenwald in NW Bavaria (e.g. Behr et al. 1982; Franke 1984; Franke et al. 1995 and references therein) and was protected from erosion due to its position within a syncline located northwest of the Fichtelgebirge anticline. The nappe concept bases mainly on the observation that the Münchberg Massif shows an inverted metamorphic profile, with amphibolite-facies metamorphic rocks at the top (Hangend-Serie), intercalated by eclogites, and greenschist-facies metamorphic rocks at their base (Prasinit-Phyllit-Serie), and that the different units are separated from each other by subhorizontal mylonitic shear zones (Stettner 1960a; Behr et al. 1982).

According to the classification of the German Stratigraphic Commission (Stettner 1997), the Hangend-Serie is now called the “Stammbacher Group”, the Liegend-Serie “Marienweiher-Group”, and Randamphibolit- and Prasinit-Phyllit-Serie form the “Grünschiefer-Group”. In practice, however, this new classification is still under discussion. The traditional names are widely used and are in accordance with the definition for so-called lithodermic units, following the North American Commission on Stratigraphic Nomenclature (2005). Therefore, the traditional nomenclature is used in the present study.

The central part of the Münchberg Massif is formed by the Hangend- and Liegend-Series, whereas the Randamphibolit- and Prasinit-Phyllit-Series are exposed only along the southwestern and southeastern margins (Fig. 1). Amphibolite-facies metamorphic overprint in the three uppermost units occurred at c. 380 Ma, as constrained by K-Ar and Ar-Ar ages of white micas and hornblende (Kreuzer et al. 1989; Kreuzer and Seidel 1989). White micas from the Prasinit-Phyllit-Serie yield consistently younger K-Ar ages of c. 365 Ma (Kreuzer et al. 1989, 1993) and Ar-Ar ages of 368-374

Ma (Kreuzer and Seidel unpubl. data), indicating juxtaposition with the other units of the Münchberg Massif during the Late Devonian. Several eclogite bodies are located at the boundary between the Hangend- and Liegend-Serie. The eclogite-facies metamorphic overprint of these bodies occurred between 405 ± 7 and 384 ± 2 Ma as suggested by Lu-Hf, Sm-Nd- and Rb-Sr isochrone ages estimated on different eclogite types (Stosch and Lugmair 1990; Scherer et al. 2002).

2.1 Hangend-Serie

Stettner (1997) divided the Hangend-Serie into banded hornblende gneiss, amphibolite and leucocratic gneiss (so-called Grenzgneis). The banded hornblende gneiss consists of centimetre to decimetre thick layers of melanocratic, hornblende-rich and leucocratic, feldspar-quartz-rich rocks. Both the melanocratic and the leucocratic layers were interpreted as metavolcanic rocks (Stettner 1997), however, the leucocratic layers were also described as sedimentary intercalations or metamorphic segregates (e.g. Emmert and Stettner 1968). The protolith of the melanocratic layers of the banded hornblende gneiss is of calc-alkaline character (Okrusch et al. 1989). The intrusion age of this hornblende gneiss is unknown so far. The leucocratic Grenzgneis is interpreted as a metavolcanic unit by Stettner (1997). Eclogite bodies commonly occur close to, or within, the thrust zone between the Hangend-Serie and the Liegend-Serie. They were considered as part of the Hangend-Serie by e.g. Matthes et al. (1974), Stettner (most recent 1997), but interpreted as tectonic bodies by e.g. Okrusch et al. (1991), Klemd (2010). The eclogites have a MORB-type composition, and their protoliths probably were formed during ocean floor spreading at 480 ± 23 Ma, as is suggested by a 7 point Sm-Nd isochrone, geochemical data, and highly superchondritic $\varepsilon Nd_{480\ Ma}$ = +8.7 (Stosch and Lugmair 1990), but also by εHf_{400Ma} between +12.2 and +6.5 (Scherer et al. 2002).

For this study, two occurrences of the banded hornblende gneiss, one amphibolite outcrop, and several Grenzgneis occurrences were sampled. Detailed information about sample localities is given in Fig. 1 and the electronic supplement S1 (Table S1). The banded hornblende gneiss is made up of medium-grained melanocratic and leucocratic layers. The melanocratic layers bear the mineral assemblage amphibole + plagioclase + quartz ± garnet ± epidote/clinozoisite ± rare chlorite, and the leucocratic plagioclase + quartz ± amphibole ± epidote/clinozoisite ± muscovite. Amphibolites consist of amphibole + plagioclase ± quartz ± epidote/clinozoisite, and the leucocratic Grenzgneis of quartz + microcline + plagioclase + muscovite ± garnet ± epidote ± sphene.

2.2 Liegend-Serie

The Liegend-Serie consists of muscovite-biotite-paragneiss and orthogneiss (partly augengneiss), and is interpreted to represent a succession of clastic metasediments, which was intruded by S-type granites (Okrusch et al. 1990). Furthermore, granodiorite and rare Al-rich gabbro are reported (Bosbach et al. 1991). Metasedimentary rocks surrounding the orthogneiss are interpreted as being metahornfels (Emmert and Stettner 1968). Deposition ages for the paragneiss sequences are unknown and intrusion ages for the S-type granites only poorly constrained by a Rb-Sr whole-rock isochrone age at 482 ± 20 Ma (Söllner et al. 1981) and by a monazite age of 495 Ma (unpublished; mentioned in Gebauer and Grünenfelder 1979). For this study, orthogneiss samples were taken from several outcrops, comprising typical augengneiss, but also intensively sheared ultramylonitic orthogneiss crosscutting the augengneiss. In addition, paragneiss samples were taken from various outcrops (Table S1). The augengneisses are mylonitic with large, lenticularly oriented alkali-feldspar porphyroclasts in a matrix of muscovite ± biotite + alkali-feldspar + plagioclase + quartz, ± garnet in some samples. The paragneisses are characterized by a well-developed foliation defined by muscovite ± biotite-rich layers alternating with quartz-feldspar (± garnet) bearing layers.

2.3 Randamphibolit-Serie

The Randamphibolit-Serie is represented by a massive, up to 1.8 km wide complex of amphibolites, associated with very minor amounts of marble, calcsilicate rocks and supposed meta-tuff (Stettner 1960b, 1964). The amphibolites have a tholeiitic composition (Okrusch et al. 1989), and their protolith ages are unknown. Our sampling is restricted to massive amphibolites. For sample localities see Fig. 1 and Table S1. In general, four petrographically distinct types can be distinguished. Type 1 is coarse-grained, massive amphibolite (hornblende + plagioclase ± epidote ± sphene ± opaque phases) from the centre of the complex; type 2 is coarse-grained amphibolite with additional garnet; type 3 is fine-grained, well foliated amphibolite, which occurs along the borders of the coarse-grained amphibolite type-1 and in contact to the Prasinit-Phyllit-Serie; and the very rare type 4 is a light-grey, coarse-grained amphibolite within the amphibolite type-1. It contains Mg-rich colourless amphibole instead of dark-green hornblende observed in the other three varieties.

2.4 Prasinit-Phyllit-Serie

The Prasinit-Phyllit-Serie occurs along the southwestern and the southeastern margin of the Münchberg Massif. It consists of fine-grained greenschist and more massive greenstone (prasinite), which are intimately intercalated with phyllite. Locally, a gradual transition between volcaniclastic and siliciclastic rocks can be observed. The mafic metavolcanic rocks show a calc-alkaline composition (Okrusch et al. 1989). From several localities, small bodies of metagabbro are described, which occur in close association with large, tectonically dismembered serpentinite bodies (e.g. Rost 1956; Bosbach et al. 1991). Most rocks of the sequence were metamorphosed under greenschist-facies conditions. Petrographic observations, however, indicate an increase in metamorphic grade towards the southeastern margin of the Münchberg Massif reaching lower amphibolite-facies conditions.

The siliciclastic metasedimentary rocks (phyllite) are strongly affected by shearing and isoclinal folding with crenulation cleavages and mobilisation of quartz into fold hinges. Reitz and Höll (1988) constrained the deposition age by acritarchs as Cryogenian to Ediacaran (former Lower Vendian). Greenschists and phyllites were sampled from different outcrops along the southwestern and the southeastern margin of the Münchberg Massif (Table S1). The mineral assemblage of the greenschist / greenstone (prasinites) comprises chlorite + epidote + albite ± actinolite ± quartz ± calcite ± titanite. Actinolite-rich, epidote-rich and calcite-rich varieties can be distinguished. The phyllites are dominated by the mineral assemblage chlorite + muscovite + albite + quartz + graphite ± pyrite, and in many places they show quartz-feldspar-segregations. At the SE margin of the Münchberg Massif, Mn-rich garnet-bearing phyllite and hornblende-bearing greenschist are observed indicating an increase of the metamorphic conditions reaching lower amphibolite-facies conditions to the SE.

3 Geochemical characterisation

Geochemical data are given in supplement S2 (Tables S2a-d), descriptions of the analytical methods are given in supplement S4. For geochemical characterisation and identification of the geological setting the geochemical data were plotted in well-established classification schemes for igneous rocks (Figs. 2-5), keeping in mind that many of the investigated rocks were affected by a more or less intense tectono-metamorphic overprint.

3.1 Hangend-Serie

Different classification diagrams (e.g. Irvine and Baragar 1971; Jensen 1976; Le Bas et al. 1986; Pearce 1996) reveal that the amphibolites and the melanocratic layers of the banded hornblende gneiss have sub-alkaline basaltic to andesitic composition with tholeiitic to calc-alkaline trend. Within the ternary Hf-Th-Ta diagram of Wood (1980; Fig. 2a), the samples plot along a trend from calc-alkaline basaltic to E-MORB composition, which is supported by other binary and ternary diagrams for a geotectonic classification (e.g. Shervais 1982; Meschede 1986; Pearce 2008). MORB-normalised trace element patterns (Fig. 3a) show enrichment in large ion lithophile elements (LILE), particularly in Ba, a negative Nb-Ta anomaly, and high field strength elements (HFSE) and REE contents reaching from slightly enriched La, Ce, P, Nd to slightly depleted Zr, Hf, Ti, Y and Yb. The melanocratic layers of the banded hornblende gneiss from Oberkotzau are more enriched in HFSE compared to the melanocratic layers from Seulbitz and the amphibolite. Chondrite-normalised REE patterns show a fractionation within the light to middle REE from La to Tb and flat patterns for the heavy REE, with highest total REE concentrations in the Oberkotzau melanocratic layers (Fig. 3b). The leucocratic layers of the banded hornblende gneiss are dacitic to rhyolitic or trachy-andesitic in composition (e.g. Le Bas et al. 1986; Pearce 1996). In MORB-normalised and REE spidergrams (Figs. 3g, h), the leucocratic layers from Oberkotzau show similar patterns like the melanocratic layers of the same outcrop with slight depletion in HFSE and heavy REE. In contrast, leucocratic layers from Seulbitz are extremely depleted in most of the HFSE and all REE, in particular the heavy REE with chondrite-normalised values below unity. In this context it has to be considered that the geochemical patterns of the melanocratic and leucocratic layers might have been biased by segregation processes during the epidote-amphibolite facies metamorphic overprint, which affected all rocks of the Hangend-Serie (for more details see discussion).

The Grenzgneis is a sub-alkaline rhyolite with ferroan, calc-alkaline, peraluminous signature (e.g. classification diagrams after Le Bas et al. 1986; Frost et al. 2001). It obviously formed along an active continental margin (classification of Schandl and Gorton 2002; Fig. 4a). The MORB-normalised trace element patterns (Fig. 3g) are LILE enriched, while the HFSE are slightly decreasing from Nb to Yb, with pronounced negative anomalies of P and Ti. The chondrite-normalised REE patterns (Fig. 3h) show a fractionation between light REE, which decrease from Ce to Sm, a pronounced negative Eu anomaly, and slight increase for the heavy REE from Gd to Lu.

3.2 Liegend-Serie

The protoliths of the investigated orthogneisses from the Liegend-Serie were granites of peraluminous, high-K alkali-calcic to calc-alkaline composition (classified after e.g. Peccerillo and Taylor 1976; Middlemost 1994; Villaseca et al. 1998; Frost et al. 2001). All samples reveal a volcanic arc, as well as a post-orogenic signature when plotted in different discrimination diagrams (see Fig. 4b, c). These ambivalent signatures are found also in other geotectonic discrimination diagrams. The protoliths of the paragneisses of the Liegend-Serie can be classified as Fe-rich sublitharenites, which were deposited in a continental arc environment (see classification schemes of Herron 1988, and Bhatia 1983 in Fig. 5).

3.3 Randamphibolit-Serie

The protoliths of the amphibolites are subalkaline basalts with high-Mg to high-Fe tholeiitic composition, according to the classification diagrams of e.g. Irvine and Baragar (1971), Le Bas et al. (1986), Pearce (1996) and Jensen (1976). Based on trace element and REE concentrations, the amphibolite samples can also be subdivided into four geochemical groups (Figs. 3c, d), which in most cases correlate with the rock types 1 – 4, based on petrographic observations. Group 1 amphibolites are very similar in composition to N-MORB basalts, but characterised by a slight enrichment in all trace and REE elements. Trace-element and REE concentrations of group 2 amphibolites are transitional between E-MORB and OIB, with tendency to E-MORB. Group 3 amphibolites (two samples) are similar to group 1 but show depletion in middle to heavy REE and HFSE compared to group 1. Group 4 is represented by light-grey amphibolite with Mg-amphibole. These rocks have very high Mg/Fe ratio (average Mg# 0.73) compared to the dark amphibolite (average Mg# 0.50) and are strongly depleted in trace elements and REE. The trace element patterns overlap with those of primitive mantle rocks (see Figs. 3c, d). Different geotectonic classification diagrams (e.g. Wood 1980; Shervais 1982; Meschede 1986; Verma et al. 2006; Agrawal et al. 2008) provide evidence that the magmatic protoliths of the group 1 amphibolites were formed in a normal MOR setting, and those of groups 2 and 3 either in an enriched MOR (E-MORB) or in a within plate setting (OIB) (Fig. 2b). Group 4 amphibolites most likely represent relicts of early cumulates.

3.4 Prasinit-Phyllit-Serie

The basic metavolcanic rocks of the Prasinit-Phyllit-Serie have basaltic to basaltic andesite compositions. Most samples show a calc-alkaline character, but a few are tholeiitic (classification diagrams after Irvine and Baragar 1971; Jensen 1976; Le Bas et al. 1986; Pearce 1996; Wood 1980; Fig. 2c). Most of the volcanic rocks obviously formed in an island arc setting (IAB-type) as is indicated by several discrimination diagrams (Pearce and Cann 1973; Shervais 1982; Meschede 1986). This is supported by enrichment in LILE and HFSE and a pronounced negative Nb-Ta anomaly (Fig. 3e). The chondrite-normalised REE patterns of the IAB-type slightly decrease from La to Lu with flat heavy REE patterns. A few samples show enrichment in all trace elements (enriched IAB-type). Their patterns are parallel to the IAB-type but with higher absolute concentrations (Fig. 3f). A few of the tholeiitic samples reveal an N-MORB-signature, and have flat N-MORB normalised multi-element patterns with mostly weak Nb-Ta anomalies (Fig. 3e), and flat chondrite-normalised REE patterns with slight depletion of light REE compared to the heavy REE (Fig. 3f). The metagabbro (sample Bae-01-08) shows patterns, which are parallel to the IAB-type samples, even though depleted in most of the trace elements and REE (Fig. 3e, f). The protoliths of the metasedimentary rocks were Fe-rich sands (following the classification diagram of Herron 1988) that were deposited predominately in an oceanic arc setting (Fig. 5).

4 U-Pb zircon ages

A total of 913 spot analyses for U–Pb dating were carried out by LA-SF-ICP-MS (laser ablation-sector field-inductively coupled plasma-mass spectrometry) on zircon grains: 273 on grains from the Hangend-Serie, 473 on grains from the Liegend-Serie, 24 on grains from the Randamphibolit-Serie, and 143 on grains from the Prasinit-Phyllit-Serie. Prior to measurement, the internal zoning of all zircon grains was characterised by cathodoluminescence (CL) and/or back-scattered electron (BSE) imaging. Representative images of zircon grains in paragneiss samples are shown in Fig. 6, and in orthogneiss samples in supplement 4 (Figs. S1 - S4). The analytical method is that described in Gerdes and Zeh (2006, 2009; for details see also supplement 4). The results of U-Pb zircon dating (including results of standard measurements) are shown in supplement 3 (Table S3). Concordia diagrams are presented in the Figs. 7 and 8, and results of detrital zircon U-Pb dating in population density diagrams in Fig. 9 (only data with a level of concordance between 90% and 110%). A summary of all ages is given in Table 1.

4.1 Hangend-Serie

Seven samples were analysed: two samples from the melanocratic layers of the banded hornblende gneiss (HS-d, OK-18b), three from the leucocratic layers of the banded hornblende gneiss (HS-h, OK-12, MGM-5) and two from the Grenzgneis (VS-20, VS-21). Zircon grains are mostly prismatic, subhedral and slightly rounded, show an oscillatory zoning (supplement 4, Fig. S1), and have Th/U ratios mostly between 0.1 and 1.9.

Zircon grains from the banded hornblende gneiss (independent of sample locality) and the Grenzgneis mostly yield within error identical Concordia ages of c. 550 Ma (Fig. 7a-c; Table 1). Some analyses in each sample yield younger (near) concordant ages down to 500 Ma (Fig. 7a-c; Table 1). As such ages were obtained randomly from both zircon cores and rims, they rather result from Pb-loss than from new zircon growth between 550 and 500 Ma. Zircon grains from sample MGM-5 show a wide spectrum of concordant ages between 700 and 475 Ma, with pronounced age peaks at 685, 616, 563, 544 and at 484 Ma (Fig. 7b, 9a). Twelve analyses yield a Concordia age of 549.0 ± 2.6 Ma (Fig. 7b; Table 1). Considering the fact that sample MGM-5 was taken from the same outcrop in

Seulbitz like the other banded hornblende gneisses, the date of 550 Ma most likely represents the time of emplacement, whereas grains with ages > 550 are inherited, and those < 550 Ma result from partial Pb-loss.

4.2 Liegend-Serie

From this series 11 samples were analysed: five orthogneisses from the southwestern part (CW-5, CW-13, CW-23, LS-2, LS-6) and six paragneisses from the northern to northwestern part of the Münchberg Massif (MGM-2, MGM-3, MGM-6, OK-1, OK-7, OK-21). Zircon grains from the orthogneisses are euhedral, columnar to tabular with sizes varying between 40 µm (tabular grains) and 350 µm (columnar grains) (supplement 4, Fig. S2a–f). All grains show oscillatory zoning. Sample LS-6 also contains a few fractured zircon grains (Fig. S2f), and porous grains were observed in all samples (Fig. S2a, c, d). Independent of the internal zoning, about 70% of the zircon grains from the orthogneiss have Th/U ratios between 0.1 and 1.6, and 30% Th/U ratios < 0.1. The zircon grains of the paragneiss samples are subhedral, tabular and slightly rounded (Fig. S2g–r). Most grains show oscillatory zoning and Th/U ratios up to 1.9 and only a few grains have Th/U < 0.1, comprising nearly all grains with ages < 400 Ma. Some zircon grains have a patchy zoning, especially at the rim (Fig. S2g, l, m, n), while others appear spongy (Fig. S2g–i, l, m). The sizes vary from 50 to 300 µm.

Zircon grains from most orthogneiss samples reveal a bimodal age distribution with Concordia ages at c. 505 Ma and 480 Ma (Table 1; Fig. 7d-f). Only a few grains gave significantly older concordant ages at about 550 Ma or even older. The age population at 505 Ma can be found in all samples, whereas the younger population at 480 Ma is restricted to three samples (LS-6, CW-13, CW-23), and predominates in sample CW-13, forming entire grains or just rims with oscillatory zoning (Table 1; Fig. 7d-f). Both ages at 505 and 480 Ma are interpreted to reflect the time of magma emplacement. Zircon grains/domains older than 505 Ma indicate an inherited component.

The zircon grains from the six paragneiss samples show a wide age spectrum ranging from 3078 Ma to 387 Ma (Fig. 9a, b), with age clusters at 390 Ma (n = 6), 509 Ma (n = 16), 544-556 Ma (n = 54), and 595 Ma (n = 11) (Fig. 9e). Older zircon grains form small clusters at 605-634 Ma (n = 8), 663-684 Ma (n = 4), 710-765 Ma (n = 3), 880-1055 Ma (n = 4), 1278 Ma (n = 1), 1802-2070 Ma (n = 4), and 3078 Ma (n = 1). The youngest cluster is represented by metamorphic zircon grains, characterised by patchy zoning patterns (Fig. 6a-c) and very low Th/U < 0.05 (found only in the two samples OK-1 and OK-7), whereas all other clusters comprise detrital zircon grains, showing mostly oscillatory magmatic zoning, and a wide range in Th/U between 0.02 and 1.9. The youngest detrital zircon grain with magmatic zoning and Th/U = 0.84 yielded a $^{206}Pb/^{238}U$ age of 478 ± 8 Ma, and seventeen grains a slightly older Concordia age of 482.8 ± 2.0 Ma, including grains from five out of six paragneiss samples (average in Table 1). The youngest grain in sample OK-21 yields an age of 501 ± 8 Ma.

4.3 Randamphibolit-Serie

From the Randamphibolit-Serie 20 zircon grains were analysed from the amphibolite near Wirsberg (sample WIR-1). The grains are mostly rounded and their elongation varies between 70 and 250 µm; several grains are fragments. Most of the grains show oscillatory zoning (Fig. S3) and Th/U ratios between 0.12 and 0.76. A few are unzoned or exhibit patchy zoning (Fig. S3). These mostly have Th/U < 0.1. Nine analyses yield a Concordia age of 402.5 ± 3.2 Ma (Fig. 8a). One core with oscillatory zoning gave an Early Ordovician, near concordant age of 471 ± 14 Ma, and the rim of the same grain an Early Devonian near concordant age of 403 ± 7 Ma (Fig. S3c). Some other analyses yielded $^{206}Pb/^{238}Pb$ ages as old as 515 Ma (94% concordance).

4.4 Prasinit-Phyllit-Serie

Zircon grains from four samples of the Prasinit-Phyllit-Serie were analysed: two phyllites (Doe-03-02, WW-03-01), one metagabbro (Bae-01-08), and one metasomatic zoisite-phengite fels (Sb-89-14). The zircon grains of the phyllites are long prismatic, slightly rounded with subhedral shape. The length of individual grains varies between 30 and 120 µm. Most of the zircon grains show an oscillatory zoning in BSE images and have Th/U ratios between 0.25 and 2.66 (Fig. 6h-r, Table S3). The zircon grains from the metagabbro are euhedral to slightly rounded, with a pronounced oscillatory zoning (Fig. S4e, f). Many zircon grains have domains with patchy zoning. Most grains appear as fragments and show dark rims in CL images (Fig. S4e). The grain size ranges between 80 and 200 µm. The metagabbro zircon grains have Th/U ratios between 0.51 and 2.36. The metasomatic zoisite-phengite fels contains zircon grains that are prismatic and mostly euhedral with grain sizes from 100 to 300 µm (Fig. S4g–j). Oscillatory zoning is frequent but many zircon grains also show patchy zoning. Their Th/U ratios range from 0.13 to 0.93.

The zircon of the metagabbro (Bae-01-08) and the metasomatic zoisite-phengite fels (Sb-89-14) yields Early Devonian Concordia ages of 401.1 ± 1.9 Ma and 406.8 ± 1.8 Ma, respectively (Table 1, Figs. 8b, c), and two grains in the zoisite-phengite fels gave older, near concordant ages of 467 and 469 Ma. Detrital zircon grains from the phyllite sample Doe-03-02 show a wide age spectrum between 3479 and 484 Ma (Fig. 9 c, f), with a major age population at 608 Ma (n = 5). Older zircon grains have ages at 1876-1989 Ma (n = 2), 2030-2089 (n = 3), 2135-2714 Ma (n = 2), and 3479 Ma (n = 1). The youngest detrital grain with magmatic zoning and high Th/U (0.72) gave a $^{206}Pb/^{238}U$ age of 484 ± 8 Ma. The age spectrum of the phyllite sample WW-03-01 is more narrow and characterised by younger ages between 411 and 378 Ma, with a pronounced age peak at 385 Ma (n=11; Table 1, Fig. 9f). The youngest detrital zircon yielded a $^{206}Pb/^{238}U$ age of 371 ± 6 Ma (Fig. 8d).

5 Discussion

5.1 Intrusion ages of magmatic rocks

Zircon grains of all samples of the **Hangend-Serie** (mafic and leucocratic banded hornblende gneiss and Grenzgneis) gave ages of about 550 Ma (Table 1), which are interpreted to date the time of intrusion of their respective magmatic protoliths. These ages overlap with those estimated for the late stage of Cadomian magmatic arc activity along the northwestern Gondwana margin, lasting from c. 750 to 530 Ma (Linnemann et al. 2010b and references therein). Zircon grains with older ages up to 705 Ma (mostly at 620 Ma) were found only in one leucocratic gneiss sample (MGM-5, Figs. 7b, 9d). It is assumed that these older grains were formed during an earlier magmatic stage of Cadomian arc evolution, and inherited during the magmatic event at 550 Ma. Concordant ages between 550 and 500 Ma were estimated on zircon grains in nearly all samples of the Hangend-Serie, in particular in the Grenzgneis. These ages most likely result from partial Pb-loss, either caused by a tectono-metamorphic overprint during the Late Cambrian / Early Ordovician and/or during the Variscan

Orogeny. This interpretation is supported by the fact that the entire range of ages was estimated randomly from zircon cores and rims.

For the metagranites of the **Liegend-Serie** two intrusion periods, at 505-499 Ma and 485-479 Ma are substantiated (Table 1). The age of about 505 Ma was found in all samples, and the age of about 480 Ma in three of the five samples, some on zircon rims with a typical magmatic zoning (Fig S2c, f). The finding of both age groups within the same sample indicates that granites emplaced at 505 Ma became reworked during a second magmatic event at 480 Ma. This age is in good agreement with a previously obtained Rb-Sr isochrone date of 480 ± 28 Ma (Söllner et al. 1981). Almost all orthogneiss samples of the Liegend-Serie contain a minor fraction of inherited zircon grains with ages at 562-534 Ma (n = 10) and 630-617 Ma (n = 2), indicating that older Cadomian basement, similar to that exposed in the Hangend-Serie gneisses became reworked during emplacement of the granitoids of the Liegend-Serie.

The concordant age of 402.5 ± 3.2 Ma from the **Randamphibolit-Serie** is much younger than the emplacement ages of the orthogneisses in the Liegend-Serie and meta-volcanites in the Hangend-Serie (Table 1). A magmatic origin of these grains is corroborated by their oscillatory zoning and Th/U ratios > 0.1 (Fig. S3). Inherited magmatic cores with ages between 471 ± 14 and 515 ± 8 Ma provide evidence for the involvement of Cambrian to Early Ordovician matter, explained by assimilation of more ancient magmatic or clastic sedimentary rocks. It is pertinent to note that formation of the Randamphibolit protolith overlaps with the high-pressure metamorphic overprint at 405-384 Ma of the eclogite bodies, which now occur in the thrust between Liegend- and Hangend-Serie (e.g. Stosch and Lugmair 1990; Scherer et al. 2002).

Both Concordia ages of 401.1 ± 1.9 and 406.8 ± 1.8 Ma from metagabbro and zoisite-phengite-fels of the **Prasinit-Phyllit-Serie** are interpreted to reflect the time of emplacement of the respective magmatic protolith. They are significantly older than K-Ar and Ar-Ar ages between 366 ± 2 and 374 ± 1 Ma estimated on muscovite of surrounding phyllitic schists, interpreted to date the final metamorphic overprint (Kreuzer et al. 1989, Kreuzer and Seidel unpubl. data). A metasomatic origin for the zircon grains in the zoisite-phengite-fels due to blackwall reactions between mafic rock and the nearby sepentinites (see Dubińska et al. 2004) can be excluded for several reasons. Most important, zircon in the zoisite-phengite-fels shows a pronounced oscillatory zoning and Th/U >> 0.1, features typical for magmatic zircon grains (Fig. S4h, i). In contrast, zircon grains precipitated from aqueous (metasomatic) fluids under low-grade to amphibolite-facies conditions commonly show very low Th/U << 0.1, and a patchy zoning (Dubińska et al. 2004; Zeh et al. 2010; Zeh and Gerdes 2014). The two zircon grains with older ages of 467 and 469 Ma in the zoisite-phengite-fels are interpreted to be inherited during emplacement of the magmatic protolith.

5.2 Deposition age and provenance of metasedimentary rocks

Clastic metasedimentary rocks from the Liegend-Serie and Prasinit-Phyllit-Serie show partly similar, partly very distinct age spectra; Hangend- and Randamphibolit-Series do not contain any clastic metasedimentary rocks. Zircon grains in paragneisses of the **Liegend-Serie** show a wide spectrum of ages between 3078 and 385 Ma, with four major age clusters at 595 Ma, 556-544 Ma, 509 Ma and 389 Ma, and an age gap between c. 1100 and 1800 Ma (Fig. 9a, b). The four older clusters were obtained from detrital zircon grains with mostly oscillatory zoning and a wide range in Th/U (from 0.1 to 1.9), and the youngest cluster at 389 ± 3 Ma from four zircon grains/domains with metamorphic characteristics (patchy zoning, Th/U < 0.02; Fig. 6a-c, Table 1; Table S3). The youngest age overlaps with metamorphic ages of 405-378 Ma estimated for different rocks (eclogites, ortho- and paragneisses) by different techniques (Lu-Hf and Sm-Nd isochrone ages, Ar-Ar and K-Ar) from the Liegend-Serie, the Hangend-Serie and the eclogite bodies of the Münchberg Massif (Stosch and Lugmair 1990; Scherer et al. 2002; Kreuzer et al. 1989; Fig. 10). Thus it is interpreted to date the amphibolite-facies metamorphic overprint of the Liegend-Series. The youngest detrital zircon yielded an age of 478 ± 8 Ma, and this maximum deposition age overlaps, within error, with the youngest magmatic Concordia age of 482.8 ± 2.0 Ma of the Liegend Serie (Table 1). The data indicate that the protoliths of at least the sampled part of the Liegend-Serie paragneisses were deposited during the Early Ordovician, synchronous or slightly younger than the second magmatic event at 485-481 Ma. Abundant zircon grains with ages at 600-590, 550-530 and at 500-490 Ma indicate substantial reworking of Neoproterozoic to Late Cambrian magmatic basement during deposition of the Liegend-Serie paragneisses.

Detrital zircon grains from two phyllite samples of the **Prasinit-Phyllit-Serie** yield very distinct age spectra (Fig. 9c, f). Sample Doe-03-02 shows a wide spectrum of ages between 3479 and 484 Ma (similar to the Liegend-Serie paragneisses), and sample WW-03-01 a very narrow spectrum between 411 and 379 Ma, with peaks at 385 and 405 Ma (Fig. 9f, Table 1). The youngest detrital grains yielded a maximum deposition age of 484 ± 8 Ma, i.e., Early Ordovician, for sample Doe-03-02, and of 371 ± 6 Ma for sample WW-03-01 (Fig. 8d). The Late Devonian age for sample WW-03-01 is only slightly older than the mean of K-Ar muscovite data of 366 ± 2 Ma and Ar-Ar muscovite data of 374 ± 1 and 368 ± 3 Ma obtained from phyllites of this series (Kreuzer et al. 1989; Kreuzer and Seidel unpubl. data), and indicates that deposition of some sediments occurred immediately prior to the tectono-metamorphic overprint in the Prasinit-Phyllit-Serie (Fig.10). Close intercalation of metavolcanic rocks and phyllite additionally reveals that deposition of the clastic sediments was accompanied by volcanic activity. This activity occurred significantly later than intrusion of the metagabbro and zoisite-phengite-gneiss protoliths at 401-407 Ma.

The maximum deposition age of 484 ± 8 Ma for sample Doe-03-02 indicates that the Prasinit-Phyllit Serie hosts not only (meta)sedimentary rocks deposited during the Late Devonian (sample WW-03-01), but perhaps also during the Early Ordovician. The maximum deposition age and the age spectrum of sample Doe-03-02 are very similar to those in the paragneiss samples from the Liegend-Serie (Fig. 9b, c). This implies that Early Ordovician rocks became re-deposited during the Late Devonian. In this context, it is pertinent to note that some phyllites of the Prasinit-Phyllit Serie contain acritarchs of Upper Cryogenian age (Reitz and Höll 1988). These acritarchs either were also re-deposited during the Late Devonian, or the Prasinit-Phyllit-Serie hosts slivers of pelitic sediments, deposited between the Cryogenian and Late Devonian (Fig. 10).

6 Geotectonic evolution of the Münchberg Massif

6.1 Hangend- and Liegend-Series

Our new data reveal different geotectonic environments at different times for the Münchberg Massif meta-igneous and metasedimentary units. The oldest metamorphic rocks of the Münchberg Massif are exposed in the **Hangend-Serie** (Grenzgneis, amphibolite, banded hornblende gneiss) and were all emplaced at about 550 Ma. Inherited zircon grains point to a reworking of an older basement formed between 700 and 620 Ma. All rocks have calc-alkaline to tholeiitic signatures, and show pronounced negative Nb-Ta anomalies, similar to rocks formed in present-day continental magmatic arcs. For example, the geochemical patterns of the Grenzgneis are similar to rhyolites exposed along the west coast of the USA (Reagan et al. 2003) and in Japan (Mt. Wasso; Ishida et al. 1998), and the signature of most banded hornblende gneisses are comparable to basic rocks in Kamchatka (Dorendorf et al. 2000), and at the west coast USA (Reagan et al. 2003; for comparison see supplement 4, Figs. S5, S6). In contrast, the signatures of the amphibolites (and the banded hornblende gneiss from Seulbitz) overlap with such of proto-arc basalts in the Izu-Bonin island arc (Pearce et al. 1999). In this context, it is pertinent to note that the geochemical signatures of most leucocratic layers in the banded hornblende gneiss are similar to those in adjacent melanocratic layers, but at Seulbitz they show significantly depleted patterns (Fig. 3). This depletion perhaps results from melt segregation, an effect already suggested by Emmert and Stettner (1968) based on structural arguments. The observed depletion patterns are very similar to those in Paleoproterozoic migmatitic rocks of the Limpopo Belt, where leucosomes alternate with biotite- and/or hornblende-dominated mafic layers on mm to cm scale (Chavagnac et al. 1999), and in migmatised paragneisses from the North Cascades, USA (Whitney and Irving 1994; for comparison see supplement 4, Fig. S7). Nevertheless, the effect of melt segregation on the composition of most of the investigated banded hornblende gneisses from the Hangend-Serie was low, in particular as the volume of leucocratic layers is mostly less than 5 vol.% (Franz and Smelik 1995, and own field observation).

In summary, combined geochemical and geochronological data reveal that all protoliths of the Hangend-Serie were formed during subduction-related bimodal magmatism in an evolved oceanic to continental island-arc environment at 550 Ma (uppermost Ediacaran); most likely within the Avalonian-Cadomian belt located at the northern Gondwana margin between the Ediacaran and Cambrian (Nance and Murphy 1996; Zeh et al. 2001; Diaz-Garcia et al. 2010; Linnemann et al. 2010b, von Raumer et al. 2015 and references therein) – (Fig. 11a-b). In fact, the amphibolites, banded hornblende gneisses and the leucocrate Grenzgneis of the Hangend-Serie provide the first direct evidence for the existence of the Cadomian magmatic arc within the Saxothuringian Zone. So far, it was only indirectly documented by geochemical signatures of Cadomian greywackes in the Lausitz anticline in eastern Germany (Linnemann et al. 2010b), and in sedimentary rocks in the Orlica-Śnieżnik Dome in the Central Sudetes (Poland), pointing to a magmatic arc / back arc system prior to 540 Ma (Szczepański and Ilnicki 2014). An active magmatic arc system along the northern margin of Gondwana during the Neoproterozoic (c. 660 – 530 Ma) is further indicated by clastic sedimentary rocks of the Teplá-Barrandian Unit (e.g. Sláma et al. 2008, Hajná et al. 2010).Felsic metavolcanic rocks in the basement of the Eastern Pyrenees also suggest the existence of a long-lived magmatic arc / back are system between 620 and 520 Ma (Casas et al. 2015). Altogether, the Hangend-Serie fits into a framework of Cadomian basement terranes, reaching from Central Iberia via South Armorica, Massif Central, and the Saxothuringian Zone to the Bohemian Massif and some Alpine basement areas (von Raumer et al. 2015).

Metahornfels aureoles around orthogneiss of the **Liegend-Serie** indicate that deposition of siliciclastic sediments, now paragneisses, occurred prior to 505-500 Ma (first magmatic stage). Nevertheless, the finding of abundant detrital zircon grains with Early Ordovician ages in the paragneisses during this study indicate that deposition continued until < 478 ± 8 Ma, i.e. nearly contemporaneous or slightly later than the second magmatic stage in the Liegend-Serie at 485-481 Ma (Fig. 10). Geochemical data of the paragneisses reveal a continental-arc signature. The wide spectrum in ages mostly between 700 and 500 Ma, with minor fractions at 700-1100 and at > 1800 Ma (Fig. 9a, b), and the age gap between c. 1100 and 1700 Ma is a typical feature for Proterozoic sediments throughout the Saxothuringian Zone. It reflects the situation that the zircon detritus was derived from three distinct sources: (i) the Avalonian-Cadomian Belt forming an Andean-type cordillera at the northern Gondwana margin between 750 and 530 Ma, (ii) the West-African /Sahara Craton south of the cordillera consisting of Archean to Paleoproterozoic basement, and (iii) remote Grenville belts (Zeh et al. 2001; Linnemann et al. 2010a, 2010b, 2014; Drost et al. 2011). Zircon age spectra with such a gap (and a similar age distribution) are not restricted to the Saxothuringian Zone, but were obtained also from many other Proterozoic (meta)sedimentary rocks throughout Europe, e.g. from the Black Forest of the Moldanubian Zone (Kober et al. 2004), French Massif Central (Chelle-Michou et al. 2017), Armorican Massif (Ballouard et al. 2017), NW Spain (Albert et al. 2015), and Morocco (Abati et al. 2012). The abundant detrital zircon grains with ages at 520-490 Ma in the Liegend-Serie were likely derived from proximal sources, i.e. surrounding granitic orthogneisses (Table 1, Fig. 10).

The continental volcanic arc signature of the granitic orthogneisses of the Liegend-Serie was, very likely, inherited during the reworking of the Cadomian magmatic arc, which occurred during two distinct stages at 505-499 Ma and 485-481 Ma. Both stages are perhaps related to the separation of the Avalonian microterrane from the northern Gondwana margin, causing large-scale crustal thinning and mantle upwelling accompanied by crust and mantle melting and formation of rift basins (see Linnemann and Romer 2002) – (Fig. 11c-d).

This rifting event is well known also from several other units within the Saxothuringian Zone and the European Variscides. In the Saxothuringian Zone, magmatism between 505 and 480 Ma is documented by granites and rhyolites (including keratophyre and quartz keratophyre) in the Elbe Zone, Lausitz Anticline, Schwarzburg Anticline, Erzgebirge Anticline, and the Frankenwald area occurring in close vicinity to the Münchberg Massif (for data and locations see: Tichomirova 2001; Linnemann et al. 2010a, b; Höhn et al. 2017). Furthermore, it is reflected by bimodal rock suites consisting of felsic volcanics and mostly MORB-type mafic rocks, in the Vesser Zone north of the Schwarzburg Anticline (Bankwitz et al. 1994; Kemnitz et al. 2002), from calc-alkaline to alkaline volcanism in the Teplá-Barrandian Unit (Sláma et al. 2008, Žák et al. 2013), from the "Leptyno-Amphibolitic Complex", forming the base of the Upper Gneiss Unit of the French Massif Central (i.e. Briand et al. 1991; Pin and Lancelot 1982; Santallier et al. 1988; Chelle-Michou et al. 2017; Lotout et al. 2017), and from the allochthonous nappe complex in NW Spain, in particular from the Lower Ophiolitic Units (Arenas et al. 2007, 2016; Sánchez Martínez et al. 2012, 2013) and the Upper Units (Abati et al. 1999; Andonaegui et al. 2012; Arenas et al. 2016). All these rock units are interpreted to result from rift-related magmatism due to separation of the Avalonia microterrane from peri-Gondwana, leading to successive opening of the Rheic ocean (Zeh and Gerdes 2010; Linnemann et al. 2010a; Romer et al. 2010 and references therein). Notably, this rifting event occurred at the same time when the basaltic protoliths of the eclogites in the Münchberg Massif were formed in a MOR-environment at 480 ± 23 Ma (Stosch and Lugmair 1990).

6.2 Randamphibolit- and Prasinit-Phyllit-Series

Metabasitic rocks of the **Randamphibolit-Serie** show MORB-type compositions and have an age of 402 Ma (Fig. 8a; 10). Nevertheless, it remains unclear whether the emplacement age of 402 Ma is representative for all four groups of amphibolites of the Randamphibolit-Serie or just for some coarse-grained varieties. In fact, most of the coarse-grained amphibolites reveal an N-MORB signature (group 1), whereas most fine-grained, and minor coarse-grained amphibolites show an E-MORB character (groups 2 to 3). The coarse-grained light amphibolite variety (group 4) most likely represents an early cumulate within a magma chamber.

Assuming that N-MORB and E-MORB were both formed in close proximity (and contemporaneous), the E-MORB character might result from a lower degree of mantle melting at shallow level, perhaps in a domain where the mid-oceanic ridge was transect by a transform fault. In such a setting, mantle flow is reduced and the plate edges cool the mantle. Another possibility could be melting of an enriched mantle or enrichment of the melt during ascent (Pearce 2008). Alternatively, E-MORB character could also be a result of epidote formation during significant fluid-rock interaction in the course of metamorphism. Epidote can incorporate high amounts of especially LREE, which leads to an overall enrichment and may pretend an E-MORB character (Brunsmann et al. 2001). However, the random distribution of epidote/zoisite amongst the N-MORB and E-MORB samples does not support the latter interpretation. In case of an asynchronous and spatially separated formation of N- and E-MORBs, the enriched metabasalts might have been emplaced also in an intra-oceanic (OIB) setting. Whatever the exact setting was, it is very likely that the metabasites of the Randamphibolit-Serie represent remnants of the Rheic oceanic crust (Linnemann 2007; Žák and Sláma 2017), and not of the Saxothuringian ocean, which according to the model of Franke et al. (1995, 2017) formed a separate oceanic basin during the Palaeozoic.

Intrusion of mafic rocks in the Randamphibolit-Serie occurred nearly synchronous with those in the **Prasinit-Phyllit-Serie,** as is indicated by the two U-Pb ages of 407 and 401 Ma (Fig.10), but their geochemical signature is quite different. Instead of a MORB signature, metagabbros, metabasalts and metatuffs in the **Prasinit-Phyllit-Serie** show calc-alkaline to tholeiitic compositions, pointing to their formation in an (oceanic) island arc setting. Such a setting is also reflected by the composition of most of the intercalated siliciclastic sedimentary rocks (Fig. 5). The geochemical patterns of most of the “calc-alkaline” metabasites are almost identical to IAB’s of the Izu-Bonin active oceanic arc (Pearce et al. 1999), whereas more tholeiitic metabasites are very similar to basalts from East Scotia back-arc system (Fretzdorff et al. 2002; see also supplement 4, Fig. S8a).

All data in combination indicate that the Prasinit-Phyllit-Serie hosts a volcano-sedimentary succession, which was deposited in an island arc / back arc environment over a period of c. 30 Ma from the Early Devonian at 407-401 Ma (intrusion ages of the metagabbro protoliths) until the Late Devonian at 371 ± 6 Ma (maximum deposition age of phyllite). Rocks of the Prasinit-Phyllit-Serie therefore provide information about the closure of the Rheic ocean (Fig. 11e), which perhaps took place along the Intra-Rheic subduction zone postulated by Sánchez Martinez et al. (2007). Many Devonian (400-390 Ma) ophiolites throughout the European Variscides are considered to be formed along this suture zone, comprising the Purrido unit in the NW-Iberian Massif (Arenas et al. 2007; Sánchez Martinez et al. 2007), the Careón ophiolite in Galicia (Diaz Garcia et al. 1999; Pin et al. 2002; Sánchez Martinez et al. 2007), and the Ślęża ophiolite in the Bohemian Massif (Dubińska et al. 2004; Kryza and Pin 2010). Alternatively, Arenas et al. (2016) suggested that at least some of these ophiolites were formed in an ephemeral, intra-oceanic pull-apart basin at 395 Ma, resulting from dextral motions between Gondwana and Laurussia. A Late Silurian/Early Devonian arc / back arc system has already been suggested for the Mid-German Crystalline Zone, c. 200 km north of the Münchberg Massif (Zeh and Gerdes 2010). This arc / back arc system, however, does not result from intra-oceanic subduction, but from subduction of the Rheic ocean beneath the Far-Eastern Avalonian microterrane, causing opening of the Rhenohercynian basin during the Devonian to Early Carboniferous (Zeh and Gerdes 2010).

The nappe pile of the Münchberg Massif allows reconstructing the spatial-time relations between basin evolution (rifting, sedimentation) and subduction / collision (metamorphic overprint) - (Fig. 11). Deposition of the volcano-sedimentary Prasinit-Phyllit-Serie occurred contemporaneous or even later than the amphibolite-facies metamorphic overprint in the Hangend-, Liegend- and Randamphibolit-Series and the high-pressure metamorphism of the eclogites between 405 and 378 Ma (Stosch and Lugmair 1990, Scherer et al. 2002; Kreuzer et al. 1989), indicating that while sediment deposition and volcanism occurred in some parts of the Rheic ocean, older oceanic crust became deeply subducted and uplifted (Fig. 10). The position of this subduction zone is discussed controversially. While Franke (2000) and Franke et al. (2017) suggest SW-directed subduction of the Saxothuringian Zone, Kroner and Romer (2013) postulate a NE-directed subduction of the Rheic ocean beneath Laurussia (or a microterrane previously attached to Laurussia, e.g. Far Eastern Avalonia), followed (i) by SW-ward directed back-thrusting of parts of the former slab during initial Variscan shortening (in NE-SW direction), and (ii) by NW-SE directed shortening (and folding) during final Variscan collision at 350-320 Ma.

The finding of phyllites with distinct age spectra in the Prasinit-Phyllit-Serie might reflect juxtaposition of different sedimentary units (Late Devonian and Early Ordovician) during stacking of the Münchberg nappes, or a change in provenance during formation of the volcano-sedimentary succession, accompanied by the re-deposition of Early Ordovician and Ediacarian sediments. A maximum deposition age of 371 Ma, as well as K-Ar and Ar-Ar ages for metamorphism between 374 and 366 Ma indicate that juxtaposition of the Prasinit-Phyllit-Serie with rocks of the Liegend- and Hangend-Serie occurred during the Late Devonian (Fig.10).

7 Summary and Conclusions

The metasedimentary and meta-igneous rocks of the four nappe units of the Münchberg Massif formed at different time and in distinct geotectonic settings during the evolution of the Saxothuringian Zone between 550 and 370 Ma (Fig. 11).

Mafic and felsic orthogneisses of the **Hangend-Serie** result from bimodal magmatism in an evolved oceanic to continental magmatic arc setting at 550 Ma. These rocks represent relics of the Cadomian magmatic arc that formed a cordillera at the northern margin of Gondwana (Fig. 11a). They are the first direct witnesses for the existence of the Cadomian arc within the Saxothuringian Zone.

Protoliths of orthogneisses of the **Liegend-Serie** were formed by reworking of Cadomian magmatic arc crust during two distinct magmatic events at c. 505 and 480 Ma (Fig. 11c, d). Deposition of the paragneiss protoliths started prior to the magmatic events and continued at least until Early Ordovician (≤ 483 Ma), followed by an amphibolite-facies metamorphic overprint at c. 390 Ma. Both magmatic events and Early Ordovician sedimentation are related to the separation of the Avalonia microterrane from the northern Gondwana margin.

Basaltic-gabbroic protoliths of the rocks of the **Randamphibolit-Serie** and **Prasinit-Phyllit-Serie** emplaced at 407-401 Ma but in different geotectonic settings (Fig. 11e). Those from the **Randamphibolit-Serie** show N-MORB to E-MORB signatures, pointing to their formation along an oceanic spreading centre during the Early Devonian (perhaps within the Rheic ocean), whereas in the **Prasinit-Phyllit-Serie** they show calc-alkaline to tholeiitic character, suggesting formation in an intra-oceanic island arc / back arc system, perhaps being part of the Intra Rheic oceanic suture zone.

Combined geochemical, geochronological and field observations suggest that the **Prasinit-Phyllit-Serie** hosts a volcano-sedimentary sequence, which was formed over a period of 30 Ma between 407 Ma (emplacement age of metagabbro) and 371 Ma (maximum deposition age of phyllite). However, Early-Ordovician maximum deposition ages of 484 Ma, and acritarchs of Ediacaran age point to re-location of rocks from sources with a more complex history.

The geotectonic setting reflected by the four Münchberg nappe units is similar to that of many other Variscan terranes throughout Europe, indicating (i) formation of the Avalonian-Cadomian magmatic arc between 700 and 530 Ma, (ii) separation of the Avalonian microterrane from Gondwana at 505 to 480 Ma, (iii) opening of the Rheic ocean between 500 and 440 Ma, (iv) closure of the Rheic ocean by intra-oceanic subduction, and/or subduction beneath Avalonia and/or Laurussia between 425 and 370 Ma, and (v) structural-metamorphic modification of the resulting nappe pile during final Variscan shortening between 350 and 320 Ma.

Acknowledgements: We would like to thank Jens Brückmann, Julia Friedrich, Fabian Herold, John Kiwus, Laura Kuulmann, Philomena Rüttiger, Vanessa Schmelz, Lisa Schopf, Christoph Walker, Florian Bremer and Mohammed Takni who contributed with data from their BSc- or diploma-theses to this project. Excellent thin sections were prepared by Peter Späthe, Würzburg University. Linda Marko and Wolfgang Dörr are thanked for the possibility to use the lab facilities and for their comprehensive support in sample separation and analyses at the LA-ICP-MS at the Goethe-University, Frankfurt. Jiří Žák, Uwe Kroner, Ulf Linnemann and one anonymous reviewer are gratefully thanked for their careful reviews and comments, which helped to improve the manuscript. This work was partially supported by a research grant (to NK) from the Faculty of Philosophy, University of Würzburg.

References

Abati J, Dunning GR, Arenas R, Díaz García F, González Cuadra P, Martínez Catalán JR, Andonaegui P (1999) Early Ordovician orogenic event in Galicia (NWSpain): evidence from U-Pb ages in the uppermost unit of the Ordenes Complex. Earth Planet Sci Lett 165: 213–228.

Abati J, Aghzer AM, Gerdes A, Ennih N (2012) Insights on the crustal evolution of the West African Craton from Hf isotopes in detrital zircons from the Anti-Atlas belt. Precambrian Research 212: 263–274. doi: org/10.1016/j.precamres.2012.06.005.

Albert R, Arenas R, Gerdes A, Sanchez Martinez S, Fernandez-Suarez J, Fuenlabrada JM (2015) Provenance of the Variscan Upper Allochthon (Cabo Ortegal Complex, NW Iberian Massif). Gondwana Research 28: 1434–1448. doi: org/10.1016/j.gr.2014.10.016.

Agrawal S, Guevara M, Verma S (2008) Tectonic discrimination of basic and ultrabasic volcanic rocks through log-transformed ratios of immobile trace elements. International Geology Review 50: 1057–1079.

Andonaegui P, Castiñeiras P, González Cuadra P, Arenas R, Sánchez Martínez S, Abati J, Díaz García F, Martínez Catalán JR (2012) The Corredoiras orthogneiss (NW Iberian Massif): geochemistry and geochronology of the Paleozoic magmatic suite developed in a peri-Gondwanan arc. Lithos 128-131: 84–99.

Arenas R, Martinez Catalán JR, Sánchez Martínez S, Diaz Garcia F, Abati J, Fernandez-Suarez J, Andonaegui P, Gomez-Barreiro J (2007) Paleozoic ophiolites in the Variscan suture of Galicia (northwest Spain): distribution, characteristics and meaning. In: Hatcher, RD Jr, Carlson MP, McBride JH, Martinez Catalán JR (eds) 4-D Framework of Continental Crust. Geol Soc Amer Memoirs 200: 425–444.

Arenas R, Sánchez Martínez S, Díez Fernández R, Gerdes A, Abati J, Fernández-Suárez J, Andonaegui P, González Cuadra P, López Carmona A, Albert R, Manuel Fuenlabrada J, Rubio Pascual FJ (2016) Allochthonous terranes involved in the Variscan suture of NW Iberia: A review of their origin and tectonothermal evolution. Earth-Sci Reviews 161: 140–178.

Bankwitz P, Bankwitz E, Kramer W, Pin C (1994) Early Paleozoic bimodal volcanism in the Vesser area, Thuringian Forest, eastern Germany. Z Geol Paläontol I 1992: 1113-1132.

Ballouard C, Poujol M, Boulvais P, Zeh A (2017) Crustal recycling and juvenile addition during lithospheric wrenching: The Pontivy-Rostrenen magmatic complex, Armorican Massif (France), Variscan belt. Gondwana Research in press.

Bhatia MR (1983) Plate tectonics and geochemical composition of sandstones. J Geol 91: 611-627.

Behr HJ, Engel W, Franke W (1982) Variscan Wildflysch and nappe tectonics in the Saxothuringian zone (Northeast Bavaria, West Germany). Amer J Sci 282: 1438-1470.

Bosbach D, Stosch HG, Seidel E (1991) Magmatic and metamorphic evolution of metagabbros in the Münchberg Massif, N.E. Bavaria. Contrib Mineral Petrol 107: 112-123.

Briand B, Piboule M, Santallier D, Bouchardon JL (1991) Geochemistry and tectonic implications of two Ordovician bimodal igneous complexes, southern French Massif Central. J Geol Soc 148: 959–971. doi: org/10.1144/gsjgs.148.6.0959.

Brunsmann A, Franz G, Erzinger J (2001) REE mobility and zoisite/fluid partitioning at near-eclogite facies conditions. Geochim Cosmochim Acta 65: 559-570.

Casas JM, Navidad M, Castiñeiras P, Liesa M, Aguilar C, Carreras J, Hofmann M, Gärtner A, Linnemann U (2015) The Late Neoproterozoic magmatism in the Ediacaran series of the Eastern Pyrenees: new ages and isotope geochemistry. Int J Earth Sci 104: 909-925.

Chavagnac V, Nägler T, Kramers JD (1999) Migmatization by metamorphic segregation at subsolidus conditions: implications for Nd-Pb isotope exchange. Lithos 46: 275-298.

Chelle-Michou C, Laurent O, Moyen JF, Block S, Paquette J-L, Couzinié S, Gardien V, Vanderhaeghe O, Villaros A, Zeh A (2017) Pre-Cadomian to late-Variscan odyssey of the eastern Massif Central, France: formation of the West European crust in a nutshell. Gondwana Research 46: 170-190.

Díaz García F, Arenas R, Martínez Catalán JR, González del Tánago J, Dunning GR (1999) Tectonic evolution of the Careón Ophiolite (northwest Spain): a remnant of oceanic lithosphere in the Variscan Belt. J. Geol. 107, 587–605.

Diaz Garcia F, Sánchez-Martinez S, Castiñeiras P, Fuenlabrada JM, Arenas R (2010) A peri-Gondwanan arc in NW Iberia. II: Assessment of the intra-arc tectonothermal evolution through U–Pb SHRIMP dating of mafic dykes. Gondwana Research 17: 352–362.

Dorendorf F, Wiechert U, Wörner G (2000) Hydrated sub-arc mantle: a source for the Kluchevskoy volcano, Kamchatka/Russia. Earth Planet Sci Lett 175: 69-86.

Drost K, Gerdes A, Jeffries T, Linnemann U, Storey C (2011) Provenance of Neoproterozoic and early Paleozoic siliciclastic rocks of the Tepla-Barrandian unit (Bohemian Massif): evidence from U–Pb detrital zircon ages. Gondwana Research 19: 213–231. doi: org/10.1016/j.gr.2010.05.003.

Dubinska E, Bylina P, Kozlowski A, Dörr W, Nejbert K, Schastok J, Kulicki C (2004) U–Pb dating of serpentinization: hydrothermal zircon from a metasomatic rodingite shell (Sudetic ophiolite, SW Poland). Chem Geol 203: 183-203.

Emmert U, Stettner G (1968) Geologische Karte von Bayern 1:25000 Blatt Nr 5737 Schwarzenbach a. d. sächs. Saale und Erläuterungen. Bayerisches Geologisches Landesamt, München.

Franke W (1984) Variszischer Deckenbau im Raume der Münchberger Gneismasse, abgeleitet aus der Fazies, Deformation und Metamorphose im umgebenden Paläozoikum. Geotekt Forsch 68: 1-253.

Franke W, Kreuzer H, Okrusch M, Schüssler U, Seidel E (1995) V.C.1 Stratigraphy, Structure, and Igneous Activity – in: Dallmeyer RD, Franke W, Weber K (eds) Pre-Permina Geology of Central and Eastern Europe. Springer, Berlin, Heidelberg, pp 277-294.

Franke W (2000) The mid-European segment of the Variscides: tectonostratigraphic units, terrane boundaries and plate tectonic evolution. In: Franke W, Haak V, Oncken O, Tanner D (eds) Orogenic processes: quantification and modelling in the Variscan belt. Geol Soc London Spec Publ 179: 35–61.

Franke W, Cocks LRM, Torsvik TH (2017) The Palaeozoic Variscan oceans revisited. Gondwana Research 48: 257-284.

Franz G, Smelik EA (1995) Zoisite-clinozoisite bearing pegmatites and their importance for decompressional melting in eclogites. Eur J Mineral 7: 1421-1436.

Franz G, Thomas S, Smith DC (1986) High-pressure decomposition in the Weissenstein eclogite, Münchberg Gneiss Massif, Germany. Contrib Mineral Petrol 92: 71-85.

Fretzdorff S, Livermore RA, Devey CW, Leat PT, Stoffers P (2002) Petrogenesis of the Back-arc East Scotia Ridge, South Atlantic Ocean. J Petrol 43: 1435-1467.

Frost BR, Barnes CG, Collins WJ, Arculus RJ, Ellis DJ, Frost CD (2001) A geochemical classification for granitic rocks. J Petrol, 42: 2033-2048. doi: 0.1093/petrology/42.11.2033.

Fuenlabrada JM, Arenas R, Fernández RD, Martínez SS, Abati J, Carmona AL (2012) Sm–Nd isotope geochemistry and tectonic setting of the metasedimentary rocks from the basal allochthonous units of NW Iberia (Variscan suture, Galicia). Lithos 148: 196-208.

Gebauer D, Grünenfelder M (1979) U-Pb zircon and Rb-Sr mineral dating of eclogites and their country rocks. Example: Münchberg Gneiss Massif, northeast Bavaria. Earth Planet Sci Lett 42: 35-44.

Gerdes A, Zeh A (2006) Combined U–Pb and Hf isotope LA-(MC)ICP-MS analyses of detrital zircons: Comparison with SHRIMP and new constraints for the provenance and age of an Armorican metasediment in Central Germany. Earth Planet Sci Lett 249: 47-61.

Gerdes A, Zeh A (2009) Zircon formation versus zircon alteration – New insights from combined U–Pb and Lu–Hf in situ LA-ICP-MS analyses, and consequences for the interpretation of Archean zircon from the Central Zone of the Limpopo Belt. Chemical Geology 261: 230-243.

Hajná J, Žák J, Kachlík V, Chadima M (2010) Subduction-driven shortening and differential exhumation in a Cadomian accretionary wedge: The Teplá-Barrandian unit, Bohemian Massif. Precam Res 176: 27-45.

Herron MM (1988) Geochemical classification of terrigenous sands and shales from core or log data. J Sed Petrol 58: 820-829.

Höhn S, Koglin N, Klopf L, Tragelehn H, Schüssler U, Frimmel HE, Zeh A, Brätz H (2017) Geochronology, stratigraphy and geochemistry of Cambro-Ordovician, Silurian and Devonian volcanic rocks of the Saxothuringian Zone in NE Bavaria (Germany) – new constraints for Gondwana break up and Rheic ocean island magmatism. Int J Earth Sci. doi: 10.1007/s00531-017-1497-2.

Irvine TN, Baragar WRA (1971) A guide to the chemical classification of the common volcanic rocks. Can J Earth Sci 8: 523-548.

Ishida H, Ishiwatari A, Kagami H (1998) The Mt. Wasso moonstone rhyolitic welded tuff in the Neogene Hokuriku Group, central Japan. J Geol Soc Japan 104: 281-295.

Jensen LS (1976) A new cation plot for classifying subalkalic volcanic rocks. Ont Div Mines Misc Paper 66: 1-21.

Kemnitz H, Romer RL, Oncken O (2002) Gondwana break-up and the northern margin of the Saxothuringian belt (Variscides of Central Europe). J Earth Sci 91: 246-259.

Klemd R (1989) P-T evolution and fluid inclusion characteristics of retrograded eclogites, Münchberg gneiss complex, Germany. Contrib Mineral Petrol 102: 221-229.

Klemd R (2010) Early Variscan allochthonous domains: the Münchberg Complex, Frankenberg, Wildenfels, and Góry Sowie. In: Linnemann U, Romer RL (eds) Pre-Mesozoic Geology of Saxo-Thuringia – From the Cadomian Active Margin to the Variscan Orogen. Schweizerbart, Stuttgart, pp 221-232.

Kober B, Kalt A, Hanel M, Pidgeon RT (2004) SHRIMP dating of zircons from high-grade metasediments of the Schwarzwald/SW-Germany and implications for the evolution of the Moldanubian basement. Contrib Mineral Petrol 147: 330–345. doi: 10.1007/s00410-004-0560-8.

Kreuzer H, Seidel E (1989) Diskrete früh-devonische Ar/Ar-Alter der Hangendserie (Münchberger Masse). Berichte Dt Mineral Ges, Eur J Mineral Bh 1: 103.

Kreuzer H, Seidel E, Schüssler U, Okrusch M, Lenz K-L, Raschka H (1989) K-Ar geochronology of different tectonic units at the northwestern margin of the Bohemian Massif. Tectonophysics 157: 149-178.

Kreuzer H, Henjes-Kunst F, Seidel E, Schüssler U, Bühn B (1993) Ar-Ar spectra on minerals from KTB and related medium-pressure units. KTB-Report 93-2: 133-136.

Kroner U, Romer R (2013) Two plates - Many subduction zones: The Variscan orogeny reconsidered. Gondwana Research 24: 298–329.

Kryza R, Pin C (2010) The Central-Sudetic ophiolites (SW Poland): Petrogenetic issues, geochronology and palaeotectonic implications. Gondwana Research 17: 292–305.

Le Bas MJ, Le Maitre RW, Streckeisen A, Zanetti B (1986) A Chemical Classification of Volcanic Rocks based on the Total Alkali-Silica Diagram. J Petrol 27: 745-750.

Linnemann U (2007): Ediacaran rocks from the Cadomian basement of the Saxo-Thuringian Zone (NE Bohemian Massif, Germany): age constraints, geotectonic setting and basin development. Geol Soc London Spec Publ 286: 35-51. doi:10.1144/SP286.4

Linnemann U, Romer RL (2002) The Cadomian Orogeny in Saxo-Thuringia, Germany: geochemical and Nd-Sm-Pb isotopic characterization of marginal basins with constraints to geotectonic setting and provenance. Tectonophysics 352: 33-64.

Linnemann U, Hofmann M, Romer RL, Gerdes A (2010a) Transitional stages between the Cadomian and Variscan orogenies: Basin development and tectono-magmatic evolution of the southern margin of the Rheic Ocean in the Saxo-Thuringian Zone (North Gondwana shelf). In: Linnemann U, Romer RL (eds) Pre-Mesozoic Geology of Saxo-Thuringia – From the Cadomian Active Margin to the Variscan Orogen. Schweizerbart, Stuttgart, pp 59-98.

Linnemann U, Romer RL, Gerdes A, Jeffries TE, Drost K, Ulrich J (2010b) The Cadomian Orogeny in the Saxo-Thuringian Zone. In: Linnemann U, Romer RL (eds) Pre-Mesozoic Geology of Saxo-Thuringia – From the Cadomian Active Margin to the Variscan Orogen. Schweizerbart, Stuttgart, pp 37-58.

Linnemann U, Gerdes A, Hofmann M, Marko L (2014) The Cadomian Orogen: Neoproterozoic to Early Cambrian crustal growth and orogenic zoning along the periphery of the West African Craton

– Constraints from U-Pb zircon ages and Hf isotopes (Schwarzburg Antiform, Germany). Precam Res 244: 236-278. doi: 10.1016/j.precamres.2013.08.007.

Lotout C, Pitra P, Poujol M, Van Den Driessche J (2017) Ordovician magmatism in the Lévézou massif (French Massif Central): tectonic and geodynamic implications. Int J Earth Sci 106: 501-515.

Maniar PD, Piccoli PM (1989) Tectonic discriminations of granitoids. Geol Soc Amer Bull 101: 635-643. doi: 10.1130/0016-7606(1989)101<0635:TDOG>2.3.CO;2.

Matthes S, Richter P, Schmidt K (1974) Die Eklogitvorkommen des kristallinen Grundgebirges in NE-Bayern - VII. Ergebnisse aus einer Kernbohrung durch den Eklogitkörper des Weißensteins. N Jahrb Mineral Abh 126: 45-86.

McDonough WF, Sun S-S (1995) The composition of the Earth. Chem Geol 120: 223-253.

Meschede M (1986) A method of discriminating between different types of mid-ocean ridge basalts and continental tholeiites with the Nb-Zr-Y diagram. Chem Geol 56: 207-218.

Middlemost EAK (1994) Naming materials in the magma/igneous rock system. Earth Sci Rev 37: 215-224. doi: 10.1016/0012-8252(94)90029-9.

Nance RD, Murphy JB (1996) Basement isotopic signatures and Neoproterozoic paleogeography of Avalonian-Cadomian and related terranes in the Circum-North Atlantic. In: Nance RD (ed) Avalonian and related peri-Gondwanan terranes of the circum-North Atlantic. Geol Soc Am Spec Pap 304: 33-346.

North American Commission on Stratigraphic Nomenclature (2005) North American Stratigraphic Code. AAPG Bull 89: 1547-1591.

Okrusch M, Seidel E, Schüssler U, Richter P (1989) Geochemical characteristics of metabasites in different tectonic units of the northeast Bavarian crystalline basement. In: Emmermann R, Wohlenberg J (eds) The German Continental Deep Drilling Program (KTB), site-selection studies in the Oberpfalz and Schwarzwald. Springer, Berlin, Heidelberg pp 67-79.

Okrusch M, Schüssler U, Seidel E, Kreuzer H, Raschka H (1990) Pre- to early- Variscan magmatism in the Bohemian Massif. In: Franke W (ed) Conference on Paleozoic Orogens in Central Europe - Geology and Geophysics, Field-Guide, Göttingen-Giessen, pp 25-35.

Okrusch M, Matthes S, Klemd R, O´Brian PJ, Schmidt K (1991) Eclogites at the north-western margin of the Bohemian Massif: A review. Eur J Mineral 3: 707-730.

Pearce JA (1996) A user's guide to basalt discrimination diagrams. In: Wyman DA (ed) Trace Element Geochemistry of Volcanic Rocks: Applications for Massive Sulphide Exploration. Geol Ass Can Short Course Notes 12: 79–113.

Pearce JA (2008) Geochemical fingerprinting of oceanic basalts with applications to ophiolite classification and the search for Archean oceanic crust. Lithos 100: 14–48.

Pearce JA, Cann JR (1973) Tectonic setting of basic volcanic rocks determined using trace element analyses. Earth Planet Sci Lett 19: 290-300.

Pearce JA, Harris NW, Tindle AG (1984) Trace element discrimination diagrams for the tectonic interpretation of granitic rocks. J Petrol 25: 956-983.

Pearce JA, Kempton PD, Nowell GM, Noble SR (1999) Hf-Nd Element and Isotope Perspective on the Nature and Provenance of Mantle and Subduction Components in Western Pacific Arc-Basin Systems. J Petrol 40: 1579-1611.

Peccerillo A, Taylor SR (1976) Geochemistry of Eocene calc-alkaline volcanic rocks from the Kastamonu area, Northern Turkey. Contrib Mineral Petrol 58: 63-81.

Pin C, Lancelot J (1982) U-Pb dating of an Early Paleozoic bimodal magmatism in the French Massif Central and of its further metamorphic evolution. Contrib Mineral Petrol 79: 1–12.

Pin C, Paquette JL, Santos Zalduegui JF, Gilbarguchi JI (2002) Early Devonian supra-subduction zone ophiolite related to incipient collisional processes in the Western Variscan Belt: The Sierra de Careón unit, Órdenes Complex, Galicia. In: Martinez Catalán JR, Hatcher RD Jr, Arenas R, Diaz Garcia F (eds) Variscan–Appalachian Dynamics: the Building of the Late Paleozoic Basement. Geological Society of America, Special Papers 364: 57–71.

Reagan MK, Sims KWW, Erich J, Thomas RB, Cheng H, Edwards RL, Layne G, Ball L (2003) Time-scales of Differentiation from Mafic Parents to Rhyolite in North American Continental Arcs. J Petrol 44: 1703-1726.

Reitz E, Höll R (1988) Jungproterozoische Mikrofossilien aus der Habachformation in den mittleren Hohen Tauern und dem nordostbayerischen Grundgebirge. JB Geol Bundesanstalt Wien 131/2: 329-340.

Romer RL, Linnemann U, Plessen B (2010) Geochemical character of the Saxo-Thuringian crust. In: Linnemann U, Romer RL (eds) Pre-Mesozoic Geology of Saxo-Thuringia – From the Cadomian Active Margin to the Variscan Orogen. Schweizerbart, Stuttgart, pp 29-34.

Rost F (1956) Ultrabasische Gesteine in der Münchberger Gneismasse. Geologica Bavarica 27: 175-231.

Sánchez Martinez S, Arenas R, Diaz Garcia F, Martinez Catalán JR, Gómez Barreiro J, Pearce J (2007). The Careón Ophiolite, NW Spain: supra-subduction zone setting for the youngest Rheic Ocean floor. Geology 35: 53–56.

Sánchez Martínez S, Gerdes A, Arenas R, Abati J (2012) The Bazar Ophiolite of NW-Iberia: a relic of the Iapetus-Tornquist Ocean in the Variscan suture. Terra Nova 24: 283–294.

Sánchez Martínez S, Arenas R, Albert R, Gerdes A, Potrel A (2013) Detailed re-dating of the Vila de Cruces Ophiolite (allochthonous complexes of NW-Iberia): The opening of a back-arc basin in the Gondwana shelf. In: Žák J, Zulauf G, Röhling H-G (eds) Crustal Evolution and Geodynamic Processes in Central Europe. Proceedings of the Joint Conference of the Czech and German Geological Societies, Pilsen, Czech Republic, p. 95.

Santallier D, Briand B, Menot RP, Piboule M (1988) Les complexes leptyno-amphiboliques (C.I.A.); revue critique et suggestions pour un meilleur emploi dece terme. Bulletin de la Societe Geologique de France IV: 3–12. doi: org/10. 2113/gssgfbull.IV.1.3.

Schandl ES, Gorton MP (2002) From continents to island arcs: A geochemical index of tectonic setting for arc-related and within-plate felsic to intermediate volcanic rocks. Can Mineral 38: 1065-1073.

Scherer E, Mezger K, Münker C (2002) Lu-Hf ages of high presure metamorphism in the Variscan fold belt of southern Germany. Gechim Cosmochim Acta 66: A667.

Shervais JW (1982) Ti–V plots and the petrogenesis of modern and ophiolitic lavas. Earth Planet Sci Lett 59: 101–118.

Sláma J, Dunkley DJ, Kachlík V, Kusiak MA (2008): Transition from island-arc to passive setting on the continental margin of Gondwana: U-Pb zircon dating of Neoproterozoic metaconglomerates from the SE margin of the Teplá-Barrandian Unit, Bohemian Massif. Tectonophys 461: 44-59.

Söllner F, Köhle, H, Müller-Sohnius D (1981) Rb-Sr Altersbestimmungen an Gesteinen der Münchberger Gneismasse, NE Bayern, Teil 1, Gesamtgesteinsdatierungen. N Jb Mineral Abh 141: 90-112.

Stettner G (1960a) Über Bau und Entwicklung der Münchberger Gneismasse. Geol Rundsch 49: 350-375.

Stettner G (1960b) Geologische Karte von Bayern 1:25000 Blatt Nr 5836 Münchberg und Erläuterungen. Bayerisches Geologisches Landesamt, München.

Stettner G (1964) Geologische Karte von Bayern 1:25000 Blatt Nr 5837 Weißenstadt und Erläuterungen. Bayerisches Geologisches Landesamt, München.

Stettner G (1997) 4.3. Münchberger Kristallinkomplex In: Stratigraphische Kommission Deutschlands (ed) Stratigraphie von Deutschland II Ordovizium, Kambrium, Vendium, Riphäikum, Teil I: Thüringen, Sachsen, Ostbayern. Cour. Forsch.-Inst. Senckenberg 200: 104-113.

Stosch H-G, Lugmair GW (1990) Geochemistry and evolution of MORB-type eclogites from the Münschberg massif, southern Germany. Earth Planet Sci Lett 99: 230-249.

Sun S-S, McDonough WF (1989) Chemical and isotopic systematics of oceanic basalts: implications for mantle composition and processes. Geol Soc London Spec Publ 42: 313-345.

Szczepański J, Ilnicki S (2014) From Cadomian arc to Ordovician passive margin: geochemical records preserved in metasedimentary successions of the Orlica Snieznik Dome in SW Poland. Int J Earth Sci 103: 627-647.

Tichomirova M (2001) Die Gneise des Erzgebirges – hochmetamorphe Äquivalente von neoproterozoisch – frühpaläozoischen Grauwacken und Granitoiden der Cadomiden. Habil. Thesis, TU Freiberg, 222 pp.

Verma SP, Guevara M, Agrawal S (2006) Discriminating four tectonic settings: Five new geo-chemical diagrams for basic and ultrabasic volcanic rocks based on log-ratio transformation of major-element data. J Earth System Sci 115: 485-528. doi: 0.1007/BF0270290.

Villaseca C, Barbero L, Herreros V (1998) A re-examination of the typology of peraluminous granite types in intracontinental orogenic belts. Transact Royal Soc Edinburgh, Earth Sci 89: 113-119.

von Raumer JF, Stampfli GM, Arenas R, Martínez SS (2015) Ediacaran to Cambrian oceanic rocks of the Gondwana margin and their tectonic interpretation. Int J Earth Sci 104: 1107-1121. doi: 10.1007/s00531-015-1142-x.

Walter R (2003) Erdgeschichte: die Entstehung der Kontinente und Ozeane. de Gruyter, Berlin.

Whitney DL, Irving AJ (1994) Origin of K-poor leucosomes in a metasedimentary migmatite complex by ultrametamorphism, syn-metamorphic magmatism and subsolidus processes. Lithos 32: 173-192.

Wood DA (1980) The application of a Th-Hf-Ta diagram to problems of tectonomagmatic classification and to establishing the nature of crustal contamination of basaltic lavas of the British Tertiary volcanic province. Earth Planet Sci Lett 50: 11-30.

Žák J, Sláma J (2017) How far did the Cadomian 'terranes' travel from Gondwana during early Palaeozoic? A critical reappraisal based on detrital zircon geochronology. Int Geol Rev: doi.org/10.1080/00206814.2017.1334599.

Žák J, Kraft P, Hajná J (2013) Timing, styles and kinematics of Cambro-Ordovician extension in the Teplá-Barrandian Unit, Bohemian Massif, and its bearing on the opening of the Rheic Ocean. Int J Earth Sci 102: 415-433.

Zeh A, Brätz H, Millar IL, Williams IS (2001) A combined zircon SHRIMP and Sm-Nd isotope study on high-grade paragneisses from the Mid-German Crystalline Rise: Evidence for northern Gondwanan and Grenvillian provenance. J Geol Soc London 158: 983-994.

Zeh A, Gerdes A (2010) Baltica- and Gondwana-derived sediments in the Mid-German Crystalline Rise (Central Europe): implications for the closure of the Rheic ocean. Gondwana Research 17: 254-263. doi: 10.1016/j.gr.2009.08.004

Zeh A, Gerdes A, Will TM, Frimmel H (2010) Hafnium isotope homogenization during metamorphic zircon growth in amphibolite-facies rocks, examples from the Shackleton Range (Antarctica). Geochim Cosmochim Acta 74: 4740-4758.

Zeh A, Gerdes A (2014) HFSE-transport and U-Pb-Hf isotope homogenization mediated by Ca-bearing aqueous fluids at 2.04 Ga: constraints from zircon, monazite, and garnet of the Venetia Klippe, Limpopo Belt, South Africa. Geochim Cosmochim Acta 138: 81-100.

Figure captions

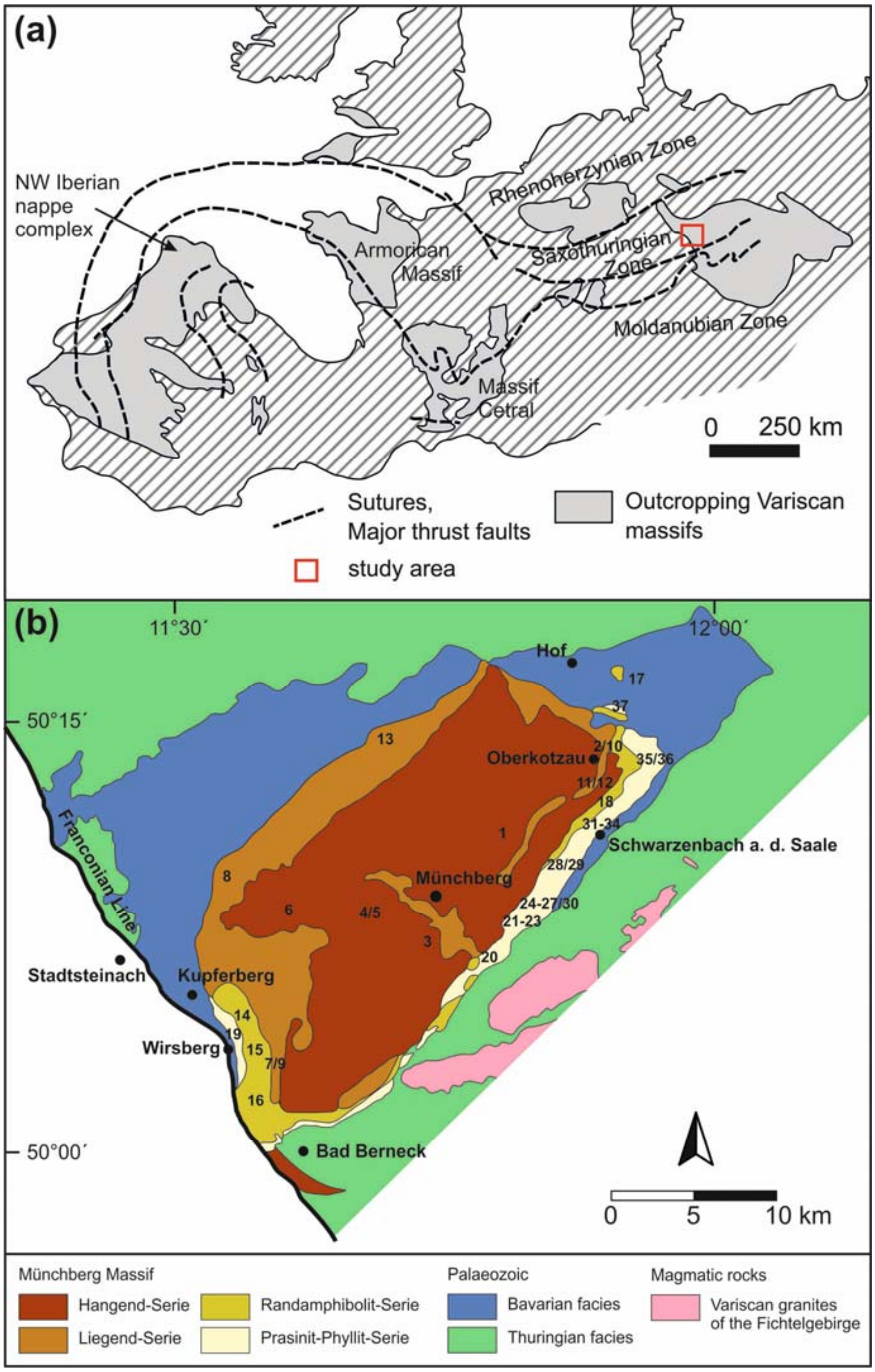

Fig. 1 Sketch map (a) showing the distribution of the outcropping Variscan massifs within Europe (after Walter 2003, Arenas et al. 2007, Fuenlabrada et al. 2012) and the location of the study area. Geological map (b) of the Münchberg Massif and the surrounding Palaeozoic rocks (modified after Kreuzer et al. 1989). Sample localities are Seulbitz (1), Oberkotzau (2, 10), Kleinlosnitz (3), Solg (4, 5), Koser Valley Marktleugast (6), Thalmühle Marktschorgast (7), Rehmühle Grafengehaig (8), Grundmühle Schorgast Valley (9), Fattigau (11, 12, 18), Schauenstein (13), Koser Valley Adlerhütte

(14), Schorgast Valley Wirsberg (15), railway cut Marktschorgast (16), Wartturmberg Hof (17), Koser Valley Adlerstein (19), Sparneck (20), Benk (21-23), Förmitz-Götzmannsgrün (24-27, 30), Förbau (28, 29), Schwarzenbach/Saale (31-34), Wurlitz (35, 36), Tauperlitz (37); numbers refer to locations in electronic supplement Table S1.

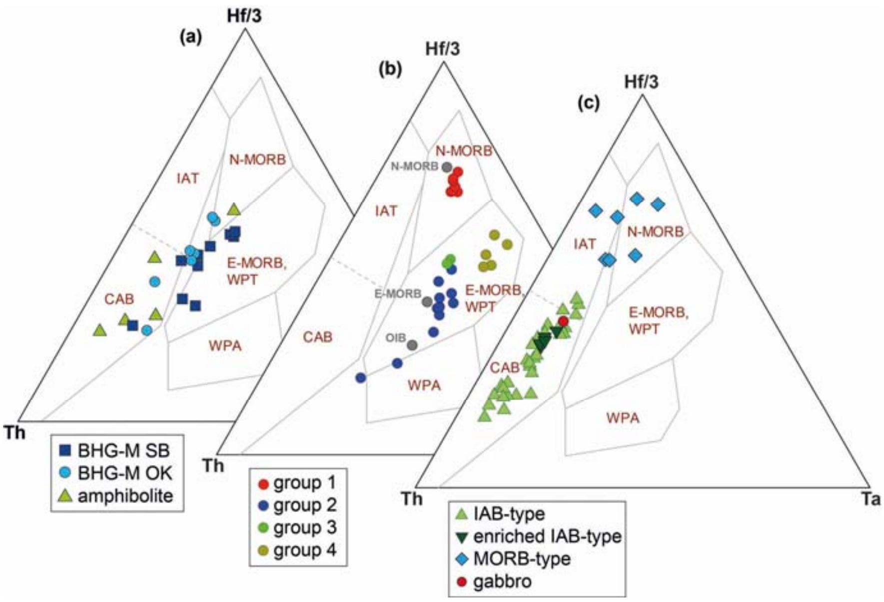

Fig. 2 Geotectonic discrimination after Wood (1980). (a) Melanocratic layers of the banded hornblende gneiss (BHG-M) from two representative outcrops (SB = Seulbitz, OK = Oberkotzau) and the amphibolite from the Hangend-Serie, (b) amphibolite from the Randamphibolit-Serie, (c) greenschist from the Prasinit-Phyllit-Serie. Abbreviations: N-MORB = normal mid-ocean ridge basalt, E-MORB = enriched mid-ocean ridge basalt, WPT = within-plate tholeiite, WPA = within-plate alkaline basalt, IAT = island-arc tholeiite, CAB = calc-alkaline basalt. Reference values for N-MORB, E-MORB and OIB are from Sun and McDonough (1989).

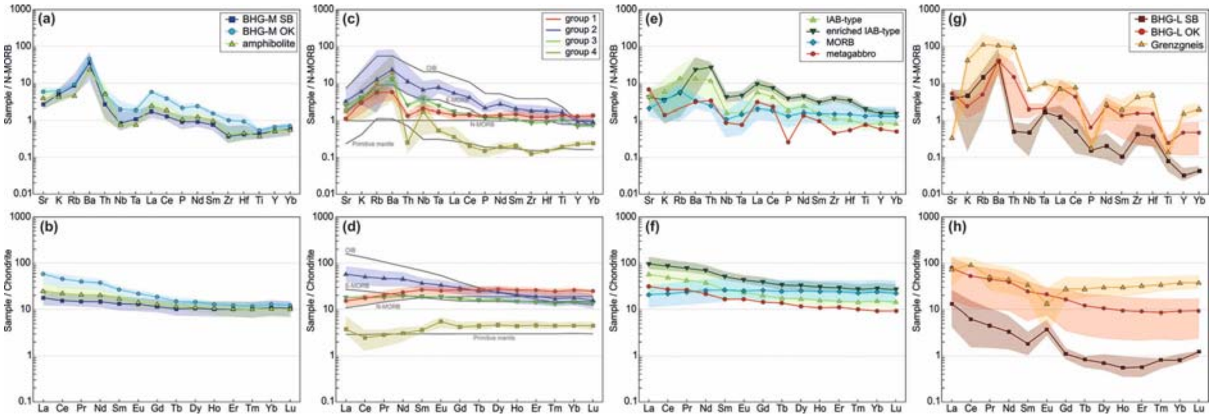

Fig. 3 N-MORB-normalised multi-element and chondrite-normalised REE diagrams of the (a, b) melanocratic layers of the banded hornblende gneiss and the amphibolitic rocks from the Hangend-Serie, the (c, d) amphibolite from the Randamphibolit-Serie, the (e, f) greenschist from the Prasinit-Phyllit-Serie, and (g, h) of the Grenzgneis and the leucocratic layers of the banded hornblende gneiss from the Hangend-Serie (BHG-L, two representative outcrops SB = Seulbitz, OK = Oberkotzau). Normalisation and reference values for N-MORB, E-MORB, OIB and PM are from Sun and McDonough (1989); normalisation values for chondrite are from McDonough and Sun (1995). Sample range of the respective group is given by the transparent area; thick line represents the average. For abbreviations see figure 2.

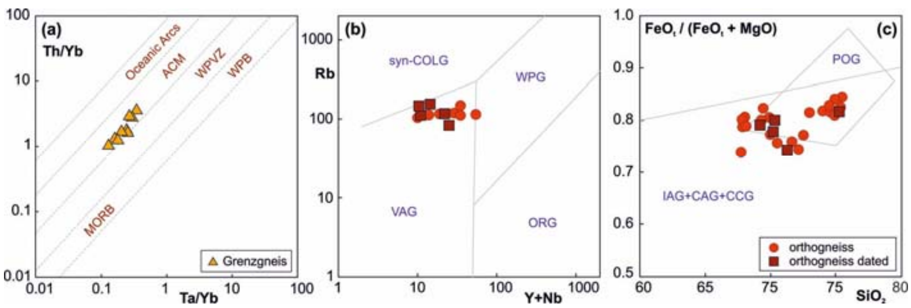

Fig. 4 Geotectonic discrimination of (a) the Grenzgneis from the Hangend-Serie after Schandl and Gorton (2002), and (b, c) of the orthogneiss from the Liegend-Serie after (b) Pearce et al. (1984) and (c) Maniar and Piccoli (1989). Abbreviations in (a): ACM = active continental margin, WPVZ = within-plate volcanic zone, MORB = mid-ocean ridge basalt, WPB = within-plate basalt. Abbreviations in (b, c): syn-COLG = syn-collision granites, WPG = within-plate granites, VAG = volcanic arc granites, ORG = ocean ridge granites, IAG = island arc granitoids, CAG = continental arc granitoids, CCG = continental collision granitoids, POG = postorogenic granitoids.

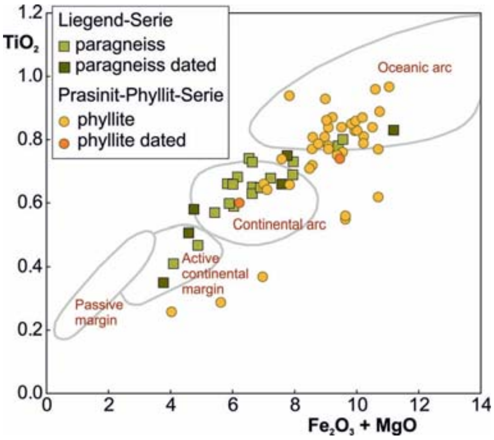

Fig. 5 Geotectonic discrimination of the paragneiss from the Liegend-Serie and the phyllite from the Prasinit-Phyllit-Serie after Bhatia (1983).

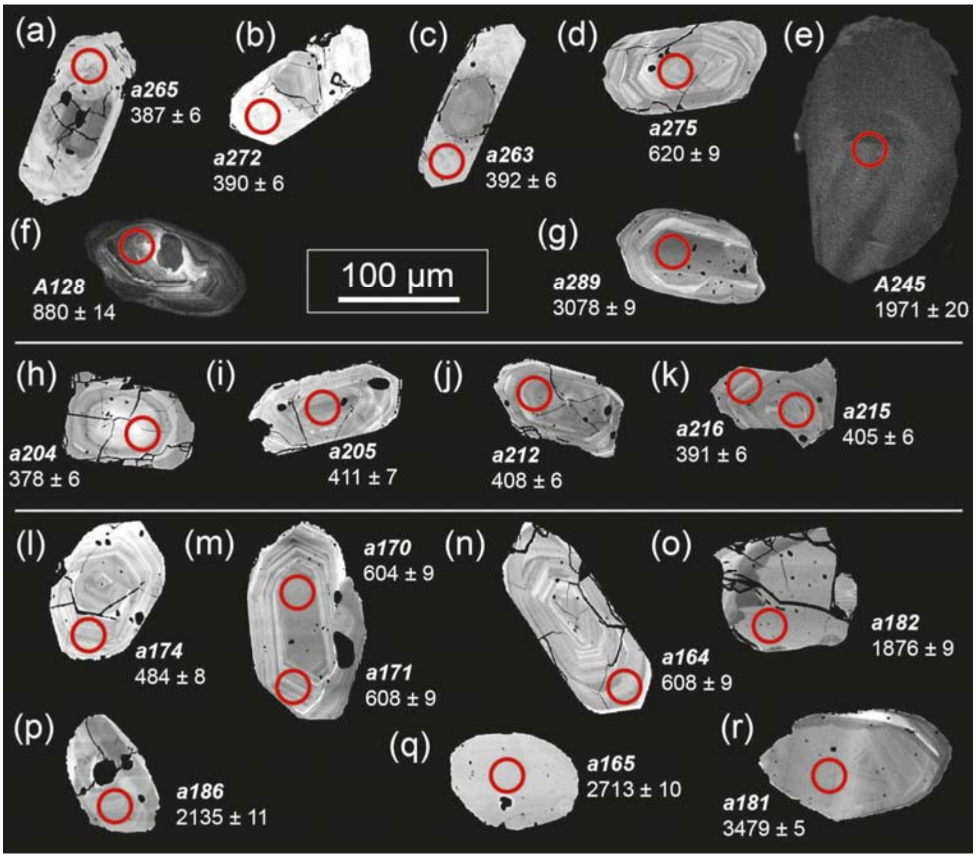

Fig. 6 Representative BSE and CL images (only e, f) of detrital zircon grains in Liegend-Serie paragneiss samples OK-1 (a-d, g), MGM-3 (e), and MGM-6 (f), and in phyllite samples of the Prasinit-Phyllit-Serie: (h-k) sample WW-03-01, (l-r) sample Doe-03-02. Spots for U-Pb measurements are indicated. Spot numbers refer to supplement S3; all presented dates < 1000 Ma are $^{206}Pb/^{238}U$ ages, and > 1000 Ma $^{206}Pb/^{207}Pb$ ages (in million years and with 2σ errors). Note, some zircon grains of sample OK-1 (a, b, c) show magmatic cores, surrounded by metamorphic rims, dating at c. 390 Ma.

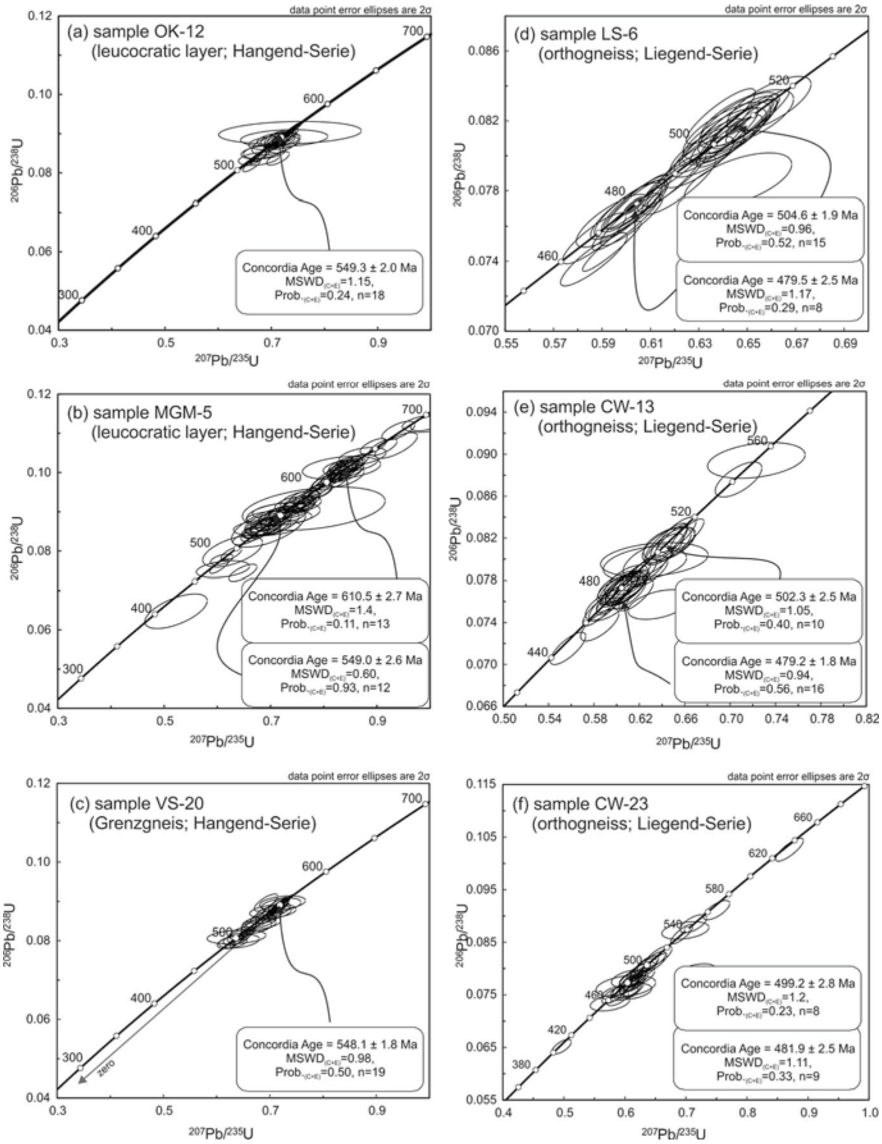

Fig. 7 Concordia diagrams showing the results of U-Pb dating of zircon in selected samples of the banded hornblende gneiss and Grenzgneis samples from the (a-c) Hangend-Serie and in orthogneiss from the (d-f) Liegend-Serie.

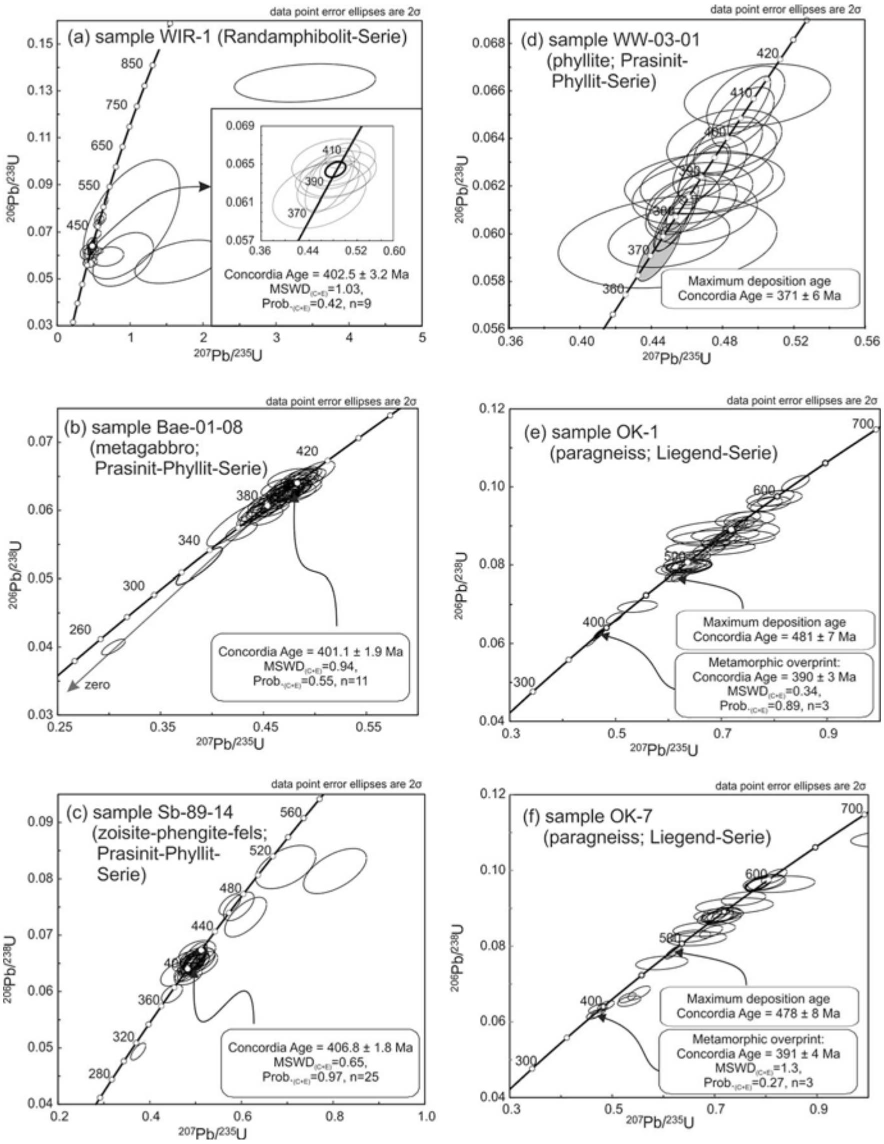

Fig. 8 Concordia diagrams showing the results of U-Pb zircon dating of (a-c) orthogneisses and (d-f) clastic metasedimentary rocks from different units of the Münchberg Massif: (a) amphibolite from the Randamphibolit-Serie; (b) metagabbro, (c) zoisite-phengite fels, and (d) phyllite from the Prasinit-Phyllit-Serie; (e-f) paragneiss from the Liegend-Serie.

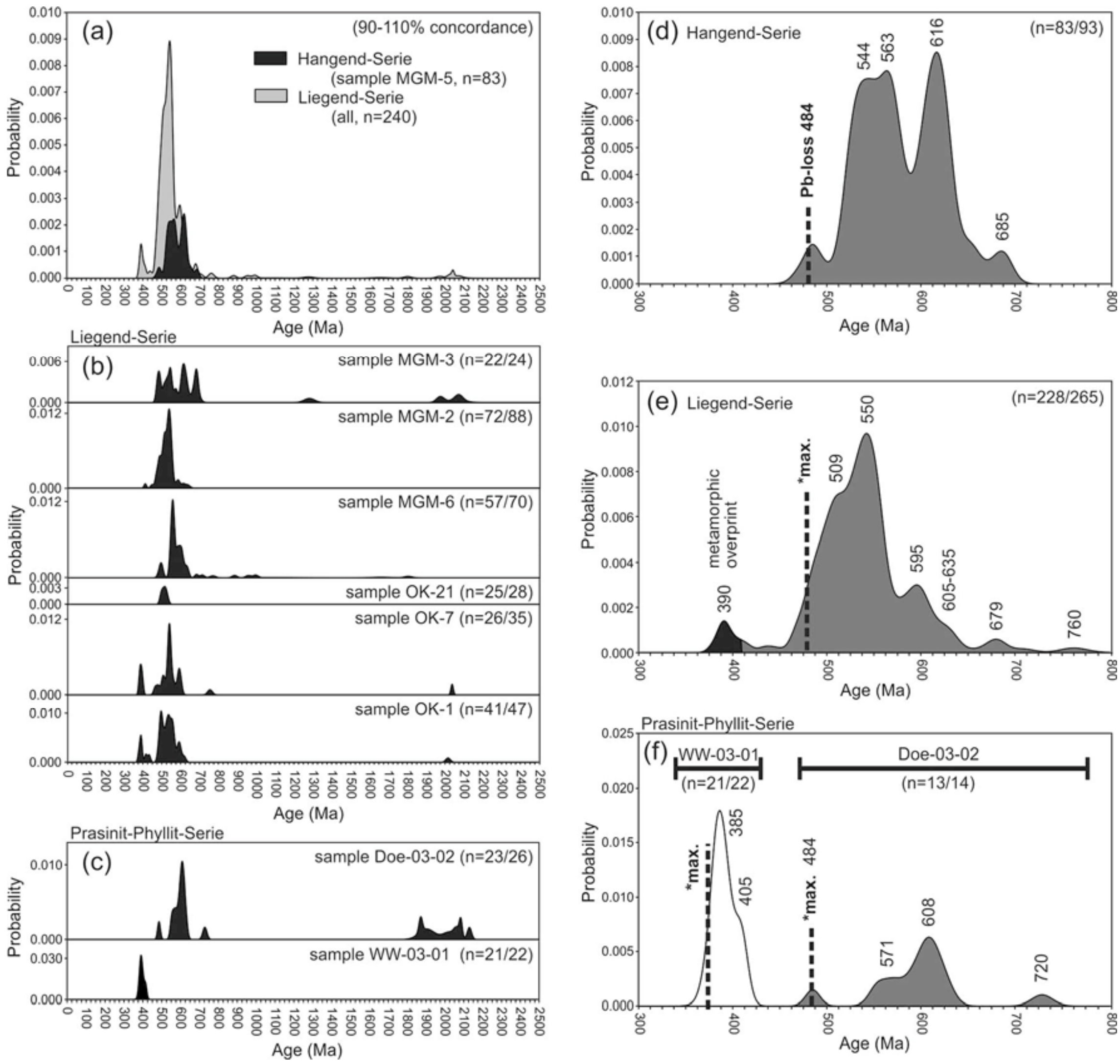

Fig. 9 Probability density diagrams showing age spectra of (a) all paragneiss samples of the Liegend-Serie and banded hornblende gneiss of the Hangend-Serie (sample MGM-5). (b-c) Results of individual paragneiss samples from the (b) Liegend-Serie, and of (c) Prasinit-Phyllit-Serie. (d-e) Enlarged spectra in the age range between 300 and 800 Ma for the (a) Hangend-Serie, (b) Liegend-Serie, and (c) Prasinit-Phyllit-Serie. *max.- maximum deposition age. For the Liegend-Serie, metamorphic zircon populations are shown in black (= metamorphic overprint). For the Prasinit-Phyllit-Serie, the two investigated samples are presented in different colours.

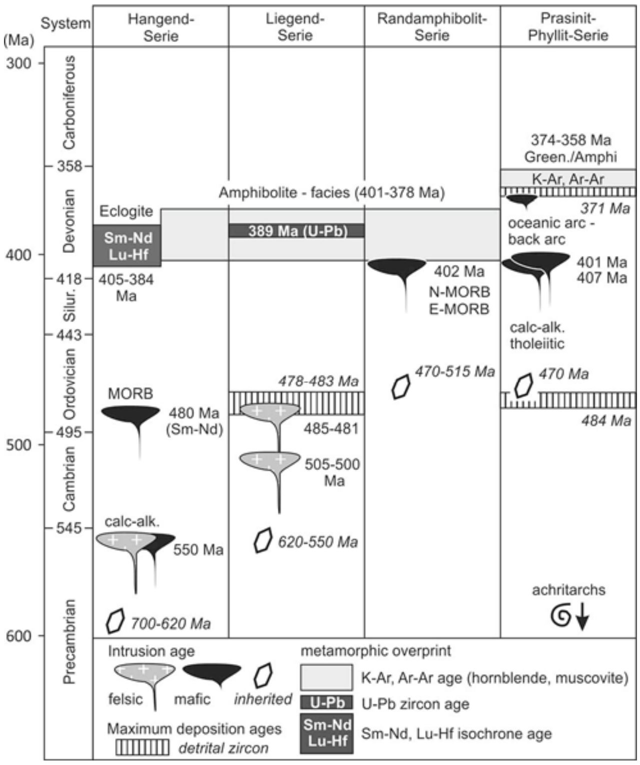

Fig. 10 Synopsis of ages estimated on orthogneisses and metasedimentary rocks of the four nappe units of the Münchberg Massif.

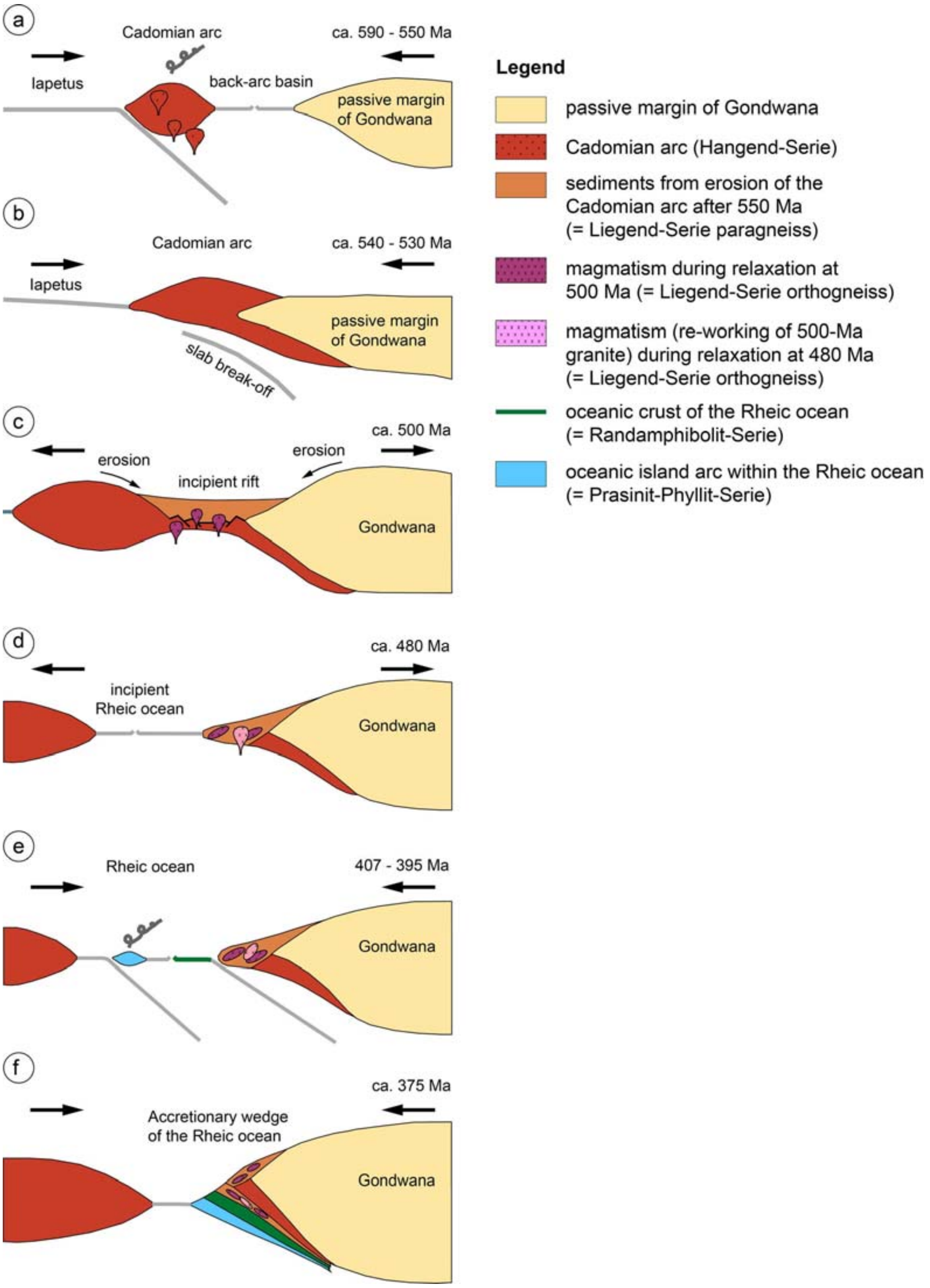

1083

1084 Fig. 11 Simplified geotectonic model showing the evolution of the four tectono-metamorphic-magmatic
1085 units of the Münchberg Massif. (a) Formation of the Hangend-Serie magmatic rocks in a late
1086 Neoproterozoic/Early Cambrian magmatic arc-back arc system along the northern margin of
1087 Gondwana. (b) Collision of the Cadomian arc, hosting the Hangend-Serie magmatic rocks, with the
1088 Gondwana passive margin until 530 Ma. (c) Late Cambrian rifting along the northern Gondwana
1089 margin leading to the erosion of the Cadomian magmatic arc, deposition of the protoliths of the

Liegend-Serie paragneisses, and intrusion of granites at 505-500 Ma (older Liegend-Serie ortho- and paragneisses). (d) Continuous rifting caused complete separation of the Avalonia microterrane from Peri-Gondwana and opening of the Rheic ocean. This stage was accompanied by sediment deposition along the northern Gondwana margin until 480 Ma and a second stage of post-Cadomian granite magmatism (younger Liegendserie ortho- and paragneisses). (e) Contemporaneous spreading and intra-oceanic closure of the Rheic ocean during the Early to Middle Devonian. Oceanic spreading is reflected by MORBs and E-MORBs of the Randamphibolit-Serie at 400 Ma, and closure by metavolcanics, greenschists and phyllites of the Prasinit-Phyllit-Serie yielding ages between 407 and 371 Ma. (f) Early Variscan stacking of the four Münchberg nappe units.

Table captions

Table 1 Summary of U-Pb ages of zircon in ortho- and paragneisses from the Münchberg Massif.

sample	AGE[1] (Ma)	±2σ (Ma)	$MSWD_{C+E}$[2]	$Prob._{C+E}$[2]	n[3] calc	n[3] total	Interpretation
Hangend-Serie (bandded hornblende gneiss and Grenzgneis)							
HS-h	550.1	2.5	0.52	0.95	10	28	intrusion
HS-d	549.8	2.5	0.96	0.51	10	21	intrusion
OK18b	551.7	1.9	0.69	0.93	20	31	intrusion
OK-12	549.3	2.0	1.15	0.24	18	36	intrusion
VS-20	548.1	1.8	0.98	0.5	19	44	intrusion
VS-21	550.0	2.7	1.2	0.24	8	23	intrusion
MGM-5	549.0	2.6	0.6	0.93	12	90	intrusion (+ inherited grains)
Liegend-Serie (orthogneiss)							
LS-2	504.0	1.8	0.8	0.82	22	28	intrusion (1st magm. event)
LS-6	504.6	1.9	0.96	0.52	15	34	intrusion (1st magm. event)
	479.5	2.5	1.17	0.29	8	34	intrusion (2nd magm. event)
CW-5	503.8	1.6	0.78	0.87	25	37	intrusion (1st magm. event)
	485.9	3.6	0.65	0.72	4	37	intrusion (2nd magm. event)
CW-13	502.3	2.5	1.05	0.4	10	39	intrusion (1st magm. event)
	479.2	1.8	0.94	0.56	16	39	intrusion (2nd magm. event)
CW-23	499.2	2.8	1.2	0.23	8	38	intrusion (1st magm. event)
	481.9	2.5	1.11	0.33	9	38	intrusion (2nd magm. event)
Liegend-Serie (paragneiss)							
OK-1	390	3	0.34	0.89	3		metamorphic overprint
	481	7			1		max. deposition age (95% conc.)
OK-7	391	4	1.3	0.27	3		metamorphic overprint
	478	8			1		max. deposition age (97% conc.)
OK21	501	8			1		max. deposition age (98% conc.)
MGM-3	480	5	1.07	0.37	3		max. deposition age
MGM-2	482	3	1.2	0.25	8		max. deposition age
MGM-6	486	6	0.72	0.61	3		max. deposition age
average	**482.8**	**2.0**	**1.1**	**0.32**	**17**		(av.) max. deposition age
Randamphibolit-Serie							
WIR-1	402.5	3.2	1.03	0.42	9	24	intrusion (+ inherited grains)
Prasinit-Phyllit-Serie (greenschist)							
Sb-89-14	406.8	1.8	0.65	0.97	25	35	intrusion (+ inherited grains)
Bae-01-08	401.1	1.9	0.94	0.55	14	52	intrusion
Prasinit-Phyllit-Serie (phyllite)							
Doe-03-02	484	8			1		max. deposition age (100% conc.)
WW-03-01	371	6			1		max. deposition age (96% conc.)
	382.2	1.9	1.1	0.34	11		max. deposition age

1) Concordia ages, except for some paragneiss samples (here deposition age)

2) MSWD and Prob. (Probability) for corncordance and equivalence (C+E)

3) calc - number used for calculation; total - number of analyses per orthogneiss sample